THE FEASIBILITY OF THE AUTOMATED VISUAL INSPECTION OF MICROCIRCUITS

BY

David A. Curtis

July 1970

Prepared Under Contract No. NAS12-2151 by

Arthur D. Little, Inc.
Cambridge, Massachusetts

Electronics Research Center
Cambridge, Massachusetts

National Aeronautics and Space Administration

Mr. Leonard M. Pauplis

Technical Monitor

NAS12-2151

Electronics Research Center
575 Technology Square
Cambridge, Massachusetts

CONTENTS

TABLES

FIGURES

THE FEASIBILITY OF THE AUTOMATED VISUAL INSPECTION OF MICROCIRCUITS

BY

David A. Curtis

Arthur D. Little, Inc.
Cambridge, Massachusetts

SUMMARY

This report describes the experimental work performed to test the feasibility of the automated visual inspection of microcircuits. The equipment, the theory of operation, and its use to obtain experimental results are all discussed. The system is based on a comparison between two circuits, one being a master. Each circuit is scanned through an optical spatial filter using white light. The signal is then detected by a photo-detector, subtracted from the signal of the other circuit and the differential signal compared with a set of decision criteria (at the simplest a fixed amplitude) to check for the presence of defects. Electrical noise does not cause problems in the operation of the gear, but measurement noise caused by translational and rotational misalignment, differences in intensity, and differences in focus between the channels set a limit on the minimum size of defect visible. The main conclusions are:

1. Using the equipment, defects can be detected automatically.
2. Further work is needed to reduce the measurement noise.
3. The parts cost for a simple unit, suitable as an aid to an operator, is about $4250 without mechanical handling equipment.
4. The equipment can inspect circuits at a rate of 20 to 30 per minute, at a cost of a few cents per circuit.

Several improvements are suggested, some to improve the operation in the presence of measurement noise, and some to avoid measurement noise. The two most promising improvements are both based

on modifications to the optical filter. One is to use a multi-segment slit; the other is to scan in two orthogonal directions. Another possible improvement is to digitize and store the data so that a trial and error procedure can be used in the signal processing to look for a match between the circuits. The inspection system suggested is feasible; with further development it holds promise of detecting small defects on complex circuits.

TOP

FOREWORD

This is the final technical report covering the work performed during NASA contract NAS12-2151, awarded May 27, 1969, to investigate the feasibility of the automated visual inspection of microcircuits. The technique described here for the inspection of microcircuits originated in an idea proposed by Arthur D. Little, Inc., for the inspection of textiles, some year ago. The problems of inspecting repetitive patterns are broadly similar and the application to microcircuits was a natural extension. The method is based on a combination of optical spatial filtering and electronic signal processing.

The basic concept involves optical scanning of the object in such a way that the information of most interest (e.g., a flaw) is enhanced while the rest of the information (e.g., the structure of a perfect object) is suppressed. The object is to accomplish as much discrimination as possible in the primary sensor in order to reduce the bandwidth and the amount of information which must be considered in evaluating the object being inspected. This approach results in electronic signals which are convenient to analyze with simple circuitry.

With spatial filtering some signals comparable to the signals produced by the defects are generated by the scanning action. The sensitivity can be improved and the false alarm rate reduced by comparing the output signal to a standard, if available. This is not a limit on the flexibility of the method. With our method another integrated circuit of the same configuration (a neighbor on the wafer) can be used for the comparison. The circuits are scanned simultaneously by identical spatial filters and the output signals are compared -- subtracted in the simplest case. Identical signals, due to imperfect spatial filtering, cancel, but signals due to flaws remain, since the probability that identical flaws exist in two integrated circuits is small. Thus, the basic pattern information is further suppressed with respect to the anomalies. This approach allows the equipment to accommodate changing ambient conditions and scanning rates, thereby simplifying the total inspection system. Also, any change in the type of integrated circuit does not necessarily mean any change in the inspection apparatus. Our present breadboard equipment uses this approach exactly.

Chapter I is a general introduction to the topic of visual inspection, emphasizing the need to inspect integrated circuits, and the type of defects which must be located. The next chapter describes the technique chosen, gives the theory of signal

generation and of the noise sources which limit the sensitivity of the equipment. Chapters III and IV describe the equipment used during the experiments and the results obtained. The last two chapters review the status of the technique, its cost, range of applicability and efficiency. They also include a detailed discussion of several possible improvements to the system.

The main conclusions are that the system suggested works, at a rather low efficiency. The limitations on the operation were set by the equipment rather than by any fundamental limits. However, noise limits do exist, so any modifications to the equipment will eventually reach these. Then, it is necessary to make more basic modifications to progress further. These include possible changes to the optical filters and the incorporation of data processing techniques.

On February 28, 1970, Dr. H. Frank Eden, who had been project director to that date, took a leave of absence from Arthur D. Little, Inc. From that date, Dr. David A. Curtis has had responsibility for the progress of the contract.

CHAPTER I - INTRODUCTION

When integrated circuits were first introduced, several advantages over discrete component circuits were claimed. These advantages included:

1. lower costs associated with the batch production techniques used;
2. increased reliability, decreased equipment down time and easier maintenance;
3. savings in size and weight;
4. improved performance, especially in harsh or abnormal environments;
5. decreased power requirements and decreased cooling requirements; and
6. decreased system assembly costs.

These have been clearly demonstrated many times, but the IC producer has to be on constant guard to ensure that his product conforms. The IC production process is a complex sequence of steps and the IC's are very susceptible to the presence of chemical impurities, physical imperfections and geometrical deviations. For these reasons the yield of good circuits can be very small. A good yield is essential to be cost-competitive a good design is essential to manufacture a good product; and a good quality control system is needed to cull out the defective circuits and to maintain the image of a reliable producer.

The quality control process has several facets. It is necessary to monitor the production equipment to maintain the units at the right settings and to monitor the product so that information can be fed back to optimize the equipment settings and maintain or increase the yields. There are several aspects of quality control; these include mechanical, thermal and electrical testing and visual inspection. Also, quality control can be extended to include failure analysis. Whether the aim is to sort the IC's into categories of good or bad, or to perform failure analysis, a visual inspection of each circuit is a valuable tool. Current practice includes visual inspection of the circuits at several stages of the production. The first stage is usually a check of the wafer while the last stage is the pre-cap visual inspection. Each type of visual inspection as currently practiced requires microscopes and human operators. The process is expensive, time-consuming, tedious, quickly leading to operator fatigue and decreasing operator efficiency. Even when the operators are fresh and alert there are deviations

between the performance of different operators since each of them applies human judgment to interpret a lengthy list of defect specifications, acceptable deviations and exceptions.

The specifications used vary between manufacturers, types of circuits and eventual applications. For this reason the various interested government agencies have drawn up detailed specifications for the visual inspection of devices which they wish to procure. Whatever the source of the specification, several features are common to all of them. The detailed work of this contract has been based upon the NASA document NASA STD XX-2, which was released in draft form for advisory purposes in February 1969. Table I lists the major classes of defects as defined in this document.

Because of the many disadvantages and the expense associated with human visual inspection, it is desirable to develop an automatic visual scheme. Such a scheme should be as effective as, or better than, human operators -- fast and inexpensive. Also, it would be compatible with the philosophy of an industry already using automated production, process control, electrical testing and data acquisition techniques.

There are three main approaches to developing an automated inspection system. They are:

1. an optical inspection scheme
2. an electrical scheme, and
3. a mixed approach.

This classification is by no means unique and there are probably many other approaches. At some stage in each technique electrical signals must be produced.

The optical approaches are essentially imaging schemes where the image of each circuit is inspected. One mechanization of this approach is the so-called flicker scheme where two circuits are presented in rapid sequence to a photodetector (usually the human eye). One of the circuits is a master. Any deviations between the circuits stand out as a flickering area against a background. In practice the whole field of view flickers to a certain extent so the human operator is still needed for judgment. At the present stage, this is only an operator's aid. Another scheme which is just at this stage is one in which parts of the image are masked out by one of a sequence of masks so that specific defects are revealed or at least enhanced over the background. A more sophisticated approach is to perform an optical transform of the image and compare the transform against a standard. The most obvious way to do this is to take a

TOP

TABLE I

A LIST OF THE MAJOR TYPES OF DEFECTS

DEFINED IN NASA STD XX-2

Defect Class	Description
Scribing	Scratches, chips, attached pieces.
Oxide layer	Discoloration, mechanical perfection, deviations from design.
Diffusion faults	Lines too narrow, possible shorts, deviations from design.
Metallization	Mechanical perfection, scratches, voids, probe marks, possible shorts. stains, corrosion, eutectic formation, deviations from design.
Die mounting and orientation	Alignment, orientation, bond, presence of excess mounting material, deviations from design.
Alignment	The design must follow good design practice.
Cracks	
Wire Bonds	Bond placement, separation and integrity, wire angles and bends, formation of eutectics, deviations from design, rebonding.
Wire Routing	Wire spacings, wire crossings, possible shorts, deviations from design.
Contamination	Foreign particles, residues, corrosion, discolorations, stains.
Package Condition	Mechanical perfection, contaminants, deviations from design.

Fourier transform, using coherent light. This has already achieved limited success at the slice evaluation stage and for inspecting metallization.

The electrical inspection schemes are based on an inspection of the electrical transform of the circuits. This can be done in principle by scanning the circuits with a point scanner and converting the optical signals into electrical waveforms, which are either stored and compared with a stored master at a later stage or compared in real time with a master.

Both approaches were seriously considered. However, a "mixed" approach was eventually adopted. This approach is considered in detail in the next chapter.

In summary, a circuit is scanned by a simple spatial filter which acts to reduce the information content by removing much of the repetitive background detail. The signal is then turned into an electrical waveform, and more of the background information is suppressed by electrically filtering the signal. This leaves a signal with the defect signal enhanced against the background of unwanted information. This signal can then be compared against decision criteria to call out the presence of the defect. This type of system was chosen because it offered several advantages. It can be built from straightforward (in many cases commercially available) components; it does not have the information bandwidth or storage requirements of a point scan method; it offers the possibility of using information generated from a neighboring circuit as the master; it does not have the operation difficulties (hazards, vibration free mountings, etc.) associated with lasers; and it offers the prospect of scanning many circuits simultaneously at little increase in cost, once the mechanical handling gear is available.

CHAPTER II - THEORY OF THE AUTOMATIC VISUAL INSPECTION TECHNIQUE CHOSEN FOR DEVELOPMENT

Integrated circuits are produced using several masking steps to define the diffusion and metallization stages in the process. For this reason each circuit produced from the same set of masks aligned on the same jigs is closely similar to its fellows. In contrast to the typical printed circuit board, the layout of the electrical components on an integrated circuit is done in terms of simple geometric features. This allows the best utilization of the silicon and the masks are easier to prepare and handle. Therefore, the perfect circuit consists of a regular array of features while the defective circuit consists of the same regular array of features with one or more irregular and undesirable features scattered at random. Any automatic visual inspection scheme must be able to detect these defects in the presence of the background pattern. The system developed during this contract uses a mixture of optical and electrical processing of the information from the circuits to suppress most of the regular circuit information and to enhance the signal from the defects.

Figure 1 shows schematically the system's mode of operation. Two slits, depicted here as simple rectangles A and B, are scanned across the two identical patterns. A photo-detector behind each slit monitors the light reflected from the object and transmitted by the slit. Typical signals showing the voltage output versus slit position are shown for both A and B. Throughout this report the signal from one channel will be referred to as a signature. The two signatures are identical except for the local minimum in signature B related to the presence of the defect on pattern B. The scanning action of the slit is a simple example of spatial filtering. Those features parallel to the direction of scan produce DC outputs; that is, their presence is effectively suppressed. However, the scanning action tends to emphasize the presence of features whose major dimension is parallel to the slit. The entry of the feature into the field of view of the slit causes a rapid increase in signal level. Once the field of view is totally filled by the feature, the signal stays constant at a new DC level until the feature starts to leave the field of view, at which point the signal level decreases. Therefore, spatial filtering by the slit has suppressed part of the information furnished by the background of the circuit. The next step is to enhance the defect signal

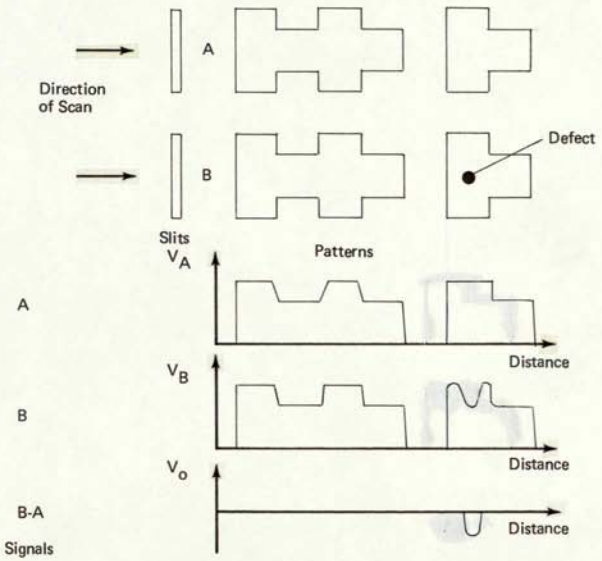

FIGURE 1 SIMPLE THEORY SHOWING THE DETECTION OF A DEFECT IN AN ITERATIVE PATTERN

by performing some electrical filtering of the signal. The most direct approach, and the one adopted during this contract, is to subtract the two signatures one from the other. This is shown in Figure 1. There, the defect is the only feature left.

Without digressing too far from the elementary theory at this stage, it is probably worthwhile to mention several difficulties immediately. The signatures of A and B are never likely to be identical and the subtraction is never likely to be perfect. Also, there are acceptable deviations between the circuits which do not represent defects. These may take the form of irregularities along the edge of a circuit after wafer dicing or as a small scratch in a harmless position on a bonding pad away from the neck of the pad. In each case, there will be a contribution to the difference signal after the subtraction, so there must be further signal processing in order to determine the presence or absence of a defect. At the simplest level, an amplitude monitor is convenient and can be used to distinguish between defect pulses and other pulses in the difference signal.

The basis of the electrical filtering technique suggested here is a comparison between two circuits being scanned simultaneously. In principle one of the circuits could be a master circuit produced especially for the job. However, there are some advantages in using parts of circuits as they become available. The only restriction is that they must be circuits of the same type. It is most unlikely that identical defects which cancel each other out will occur. However, some types of defects do have a regular nature, notably those caused by a mask misalignment, so, for 100% security, visual inspection of one circuit per wafer is necessary. If pairs of circuits are inspected as they become available, it is necessary to devise some scheme by which a defect observed by monitoring the differential channel can be assigned to one circuit or the other. Either a system which monitors the sign of the defect pulse or a majority logic system based on the scanning of three or more circuits together could be implemented. If a master circuit is permanently available these troubles do not occur. Also, the master circuit helps reduce some of the difficulties caused by gradual changes in the oxide color which affect the contrast of circuit features and cause a permanent imbalance in the differential signal.

The decision as to whether or not to use a master depends on the needs of the user and does not affect the work on the feasibility of the inspection scheme proposed here.

Theory of the Operation

The voltage output from the photo-detector can be related simply to the main parameters of the system. At a given instant

in time the light incident on the photo-detector depends on the circuit features viewed through the slit and the intensity of the incident light. In general the voltage is given by:

$$V = KI \Sigma_i A_i R_i .$$

K represents the overall efficiency of the optical system and the photo-detector; I represents the intensity of illumination on to the circuit; A_i is the area visible through the slit of circuit feature i; and R_i is the reflection coefficient of circuit feature i.

Figure 2 schematically shows two slits being scanned across two circuits; in channel B there is a defect of area Δa. The defect need not be smaller than the slit but if it is larger, Δa represents the area of the defect visible through the slit at a specified time. The differential output signal is given by:

$$V_o = KI \quad (\Sigma_i A_i R_i)_A \; - \; (\Sigma_i A_i R_i)_B = KI \Delta a \Delta R,$$

where ΔR is referred to in this report as the contrast of the defect and represents the difference in reflection coefficient between the defect and the perfect circuit feature at the same location on the other circuit. Note that this definition of contrast is not the same as the definition used in photography or illumination engineering. The basic conclusion is that the magnitude of the defect pulse in the differential signal depends on the product of the defect area and contrast, and that doubling the area of the defect while simultaneously halving the contrast gives the same value of V_o. During the derivation the assumptions listed in Table II were made. Constancy of K depends on matching the two channels in both their optical and electronic stages. Notably the gain, the f-number, and focus must be kept constant.

Figure 3 shows the relationship between the amplitude of the defect pulse in the differential signal and the diameter of a circular defect. The voltage scale is reduced by the product KI and normalized to unity for a 10 mil diameter defect of high contrast. The slit is assumed to be a rectangle measuring 50 x 0.1 mils. For defects with a diameter less than the slit width, the area of the defect seen through the slit increases as D^2; for defects with a diameter greater than the length of the slit the area viewed is constant; for defects with an intermediate diameter the area viewed goes as D. The amplitude of the defect pulse also follows these dependencies. Between the square-law and the linear region there is a short transition range. Two plots are given to indicate the dependency on ΔR, in this case: $\Delta R' = 5\Delta R''$.

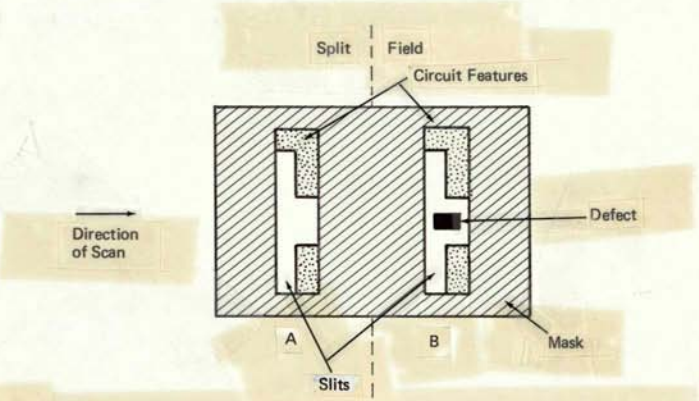

FIGURE 2 A SCHEMATIC REPRESENTATION OF TWO SLITS SCANNING OVER TWO CIRCUITS, ONE WITH A DEFECT

TABLE II

ASSUMPTIONS USED IN THE SIMPLE THEORY

- K and I are constant
- Translational and rotational alignment of the slits over the circuits is precise.
- Slits are identical.
- Circuits are identical.
- Scan speeds are identical.

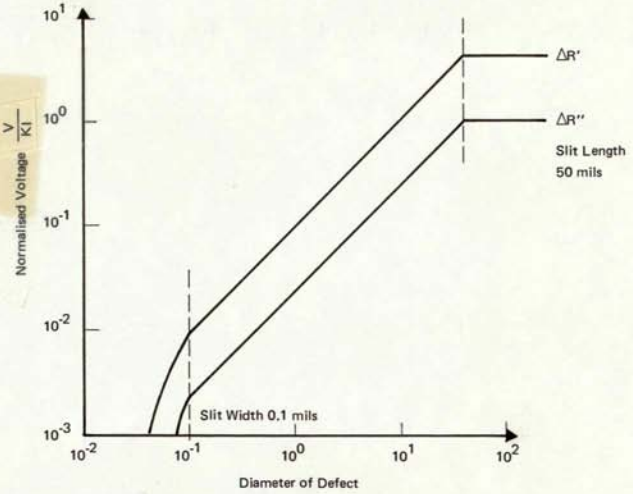

FIGURE 3 THE PEAK SIGNAL AS A FUNCTION OF DEFECT DIAMETER FROM A CIRCULAR DEFECT VIEWED THROUGH A RECTANGULAR SLIT

Noise

There are two main types of noise in the system, electrical noise and measurement noise. The former is associated with the electronic circuits, particularly the photo-detector; the latter is generated by the action of the system during an inspection. Experience gained during the experimental work indicates that measurement noise is the most important. However, electrical noise is considered first, briefly. If the signal to noise ratio S/N is limited by the detector, then:

$$\frac{S}{N} = (I\eta\Delta a\Delta R)/(NEP\ \sqrt{\Delta f})^{1},$$

where I is the illumination intensity; η is the efficiency of the optics; Δa is the area of the defect viewed through the slit; ΔR is the contrast of the defect; NEP is the noise equivalent power of the detector; and Δf is the bandwidth of the electronics.

If we assume that:

$I = 10^{2} W\ cm^{-2}$,

$\eta = 10^{-3}$,

$\Delta R = 3 \times 10^{-2}$

$NEP = 10^{-12} W\ Hz^{-\frac{1}{2}}$,

$\Delta f = 10^{4} Hz$,

and $S/N = 3$,

then Δa, the minimum area defect observable, is $10^{-7} cm^{2}$. If the defect is circular it has a diameter of 0.15 mil. In practice, the scan rate for circuits was many seconds per circuit so the required bandwidth was much less than 10kHz. Also, a photo-multiplier was used instead of a solid state photo-detector, so the noise equivalent power was much less than the value quoted here. For this reason, the electrical noise was not a problem during the experiments. The calculation given above indicates that even at a scan rate equivalent to one circuit per second, the electrical noise is not going to set a significant minimum size to the defects detectable if a good quality photomultiplier is used.

The lower limit on the size of defect set by the measurement noise is a different problem. When the two slits are not set up identically, there is an out-of-balance signal which is not related to the presence of defects on one or the other of the two circuits being scanned. This unwanted out-of-balance signal is the measurement noise which hides the genuine out-of-balance signal caused by defects.

Causes of the out-of-balance signal are given in Table III. They are illustrated in Figure 4. The sources of the measurement noise may be related to differences in f-number and focus between channels, built-in deviations of the circuits, dissimilar slits, or to inefficiencies in the alignment of the slits over the circuits. In the experimental apparatus assembled, the inefficiencies of the mechanical alignment and the differences in focus between the channels were the main limitations. Ultimately, the limitation is likely to be one of acceptable differences in reflection coefficient from point to point on the metallization.

The theoretical limits set by measurement noise in several situations will be evaluated assuming a rectangular slit of length L and width w, L>>w.

Misalignment Along the Direction of Scan, Figure 4(i). If identical features on the two circuits are separated by X and the two slits are separated by X-Δw, then one slit will reach changes in the features on the circuits before the other during the scan, giving rise to an out-of-balance signal between the two channels. This signal is given by:

$$V_o = V_A - V_B,$$

where the subscripts A and B indicate the two separate channels. The out-of-balance signal increases in size until the second slit starts to see the same feature; then it stays constant until the first slit's field of view is completely filled by the feature, or until the feature occupies the maximum area of the slit that it can attain. Then, the signal V_o will start to decrease. Let us look at the worst case, which occurs frequently. That is, the slits are passing over the circuit edge, or a major metallization feature, which can fill the whole slit at a specific time. At time t = 0 neither slit sees the metallization, therefore $V_o = 0$. At time $t = t_1$, slit A sees an area $L\Delta w$ of the metallization while slit B sees nothing; the metallization is on the point of entering the field of view. Then,

$$V_A = KI(R + \Delta R)\ L\Delta w + KIRL(w - \Delta w)$$

where R is the reflectivity of the background averaged over the slit and ΔR is the increase in reflectivity of the metallization. Also,

$$V_B = KIRLw,$$

therefore,

$$V_o = KIL\Delta R\Delta w.$$

TABLE III

CAUSES OF OUT-OF-BALANCE SIGNALS

1. Misalignments between slits.
2. Intensity differences between channels.
3. Rotations between slits.
4. Acceptable circuit deviations.
5. Defects.

1 - 4 form measurement noise; 5 is the signal.

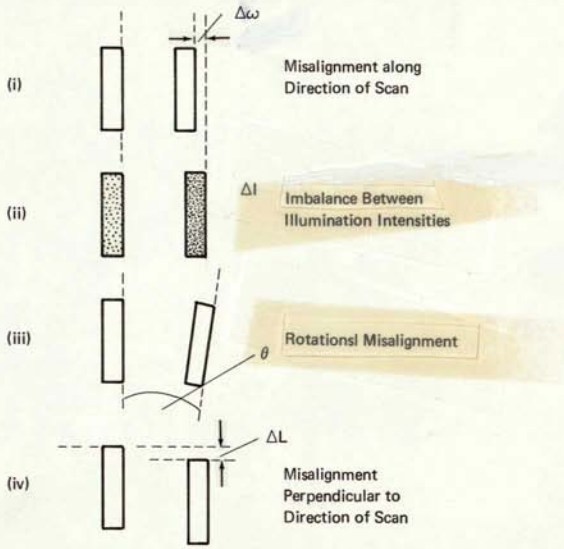

FIGURE 4 SOME SOURCES OF MEASUREMENT NOISE

Since we assume a uniform scan velocity u, the signal V_o builds up from zero linearly with time. That is, $w = ut$. This signal stays constant until slit A sees only metal, then:

$$V_1 = KI(R + \Delta R)Lw$$

and

$$V_2 = KI(R + \Delta R)L(w - \Delta w) + KIRL\Delta w.$$

therefore,

$$V_o = KIL\Delta R\Delta w,$$

as it should. After this, V_o decreases linearly with time until slit B is completely filled with metal. When the metal starts to move away from the slits, the same sequence is followed, except that the difference signal V_o is now negative.

The important thing is to set an upper limit on Δw so that reasonably small defects of contrast roughly equal to, or less than, ΔR can be seen in the difference signal V_o. A typical small defect could be a black foreign particle, D mils square, constrast ΔR, capable of bridging the spacing between two lines of metallization. For a slit of width less than D, the maximum defect signal is given by

$$V_{defect} = KI\Delta RDw.$$

The signal to noise ratio is then

$$\frac{S}{N} = \frac{V_{defect}}{V_o} = \frac{Dw}{L\Delta w} .$$

We have assumed that the contrasts ΔR cancel out, which is a convenient but unlikely approximation. Assuming S/N = 3, then

$$\Delta w = \frac{Dw}{3L}$$

is the maximum allowable misalignment in order to be able to see a defect of size D.

This relation has been derived for a simple, but frequently occuring case. By introducing three constants, α, β, and k, it can be generalized somewhat:

$$\Delta w = \alpha kwD/3\beta L.$$

α describes the modification to the area of the defect which is viewed through the slit if the defect is not square as assumed above; a square defect has $\alpha = 1$. β describes the modification which must be made if the feature which enters the slits does not occupy the whole length of the slit. This may be because it is a short feature, or because the slit scans across it at an angle, or both. k describes the ratio between the two contrasts; $k>1$ means the defect has a higher contrast than the misaligned feature in view.

Misalignment Along the Slit, Figure 4 (ii). -- The calculations for misalignment along the slit are very similar. Here the differential signal is $V_o = KIw\Delta R\Delta L$, where ΔL is the misalignment along the slit and one slit is filled with metal (for example) while the other sees metal and an area $w\Delta L$ of background. The signal to noise ratio is given by

$$\frac{V_{defect}}{V_o} = \frac{\alpha kD}{\beta \Delta L} .$$

Illumination and Focus, Figure 4 (ii). -- Illumination and focus are related, since a change in focus of one objective is really a change in the solid angle over which collection of light can occur. This alters the illumination. Alternatively stated, reflections from highlights are blurred over an area larger than the highlight on defocusing, thus reducing the beam intensity. Any discrepancy in focusing causes a fluctuating out-of-balance signal because the variations in the heights of features across the circuit, the depth of field limits, and the differences in focus interact with each other in a complex manner.

If the intensity in one channel is changed to fI, where f is the percentage of light transmitted through the slit, then

$$V_o = KRLwI(1 - f).$$

The defect signal is:

$$V_{defect} = KI\Delta RDw;$$

if the defect occurs in the channel with the higher intensity. Then:

$$\frac{V_{defect}}{V_o} = \frac{D\Delta R}{RL(1-f)}$$

The most important source of illumination problems is local variations in the reflection coefficient.

Rotations, Figure 4 (iii). -- These will not be treated in detail. Assume the example of the metallization step considered for the alignment problem with an angular misalignment between the slits of θ radians. Then:

$$\frac{V_{defect}}{V_o} = \frac{2Dw}{L^2\theta}$$

Acceptable Deviations Between Circuits. -- The tolerances of the photolithographic technique are such that there is a chance of deviation between circuits. Current practice sets the maximum deviation at 20 μin, but in many cases it is much smaller. The misalignment equations apply in this case also.

All the contributions to the signal to noise ratio may occur together. Their contributions can probably be added in a Gaussian manner to give a total misalignment of

$$\Delta w = \sqrt{\Sigma_i \Delta w_i^2}.$$

Table 4 lists side lengths for the minimum square defect which can be observed in a variety of situations. It is assumed that a signal to noise ratio of 3:1 gives an acceptably small number of false alarms due to noise spikes in the system.

The estimates in Table IV show that the most critical feature is the misalignment along the scan, followed by changes in illumination (whether caused by defocusing, lamp changes or acceptable changes in the reflectivity of parts of the circuits), rotation of one slit with respect to the other, and misalignment along the slits. Small variations between circuits caused by the photolithography process also contribute to the noise in the same order as above. Of course, the contributions from all the sources are likely to occur on each pair of circuits in an unknown and unpredictable sequence, as circuit features and defects enter and leave the field of view at random times. This means that the difference signal is the sum of a large number of terms.

The out-of-balance signal attributable to mechanical misalignments only occurs while the signal levels in one channel or the other are changing. The measurement noise from the illumination, focus, and reflection coefficient changes occurs at irregular intervals during a scan. Measurement noise has proved to be the limiting factor on the minimum size of defects seen during the course of the experiments.

The experimental scheme adopted is only one of several possible variations on the idea. A block diagram showing the main features of the system in schematic form is given in Figure 5. The notes

TABLE IV

MINIMUM OBSERVABLE SIZE OF SQUARE DEFECT

All dimensions in mil.

D is the side length of the minimum square defect.

A. Misalignment along the scan

$D = 3 \beta L \Delta w / \propto kw$

Assume $\beta / \propto k = 1$

Δw	w	L	D
0.02	0.15	15	6
0.02	0.6	15	1.5
0.04	0.6	15	3

$\beta / \propto k$ can vary between about 0.1 and 2, so D in the table above can vary between 0.15 and 12 mil.

B. Misalignment along the slit

$D = 3 \beta \Delta L / \propto k$

$\beta / \propto k$	ΔL	D
0.1	1	0.3
1	1	3
2	1	6
2	0.1	0.6

C. Intensity

$D = 3RL (1 - f)/\Delta R$

$R/\Delta R$	$(1 - f)$	L	D
1	0.03	15	1.4
1	0.01	15	0.45
4	0.01	15	1.8
4	0.001	15	0.18

continued---

TABLE IV (continued)

D. Orientation

Angles in radians

$D = 3L^2\theta/2w$

θ	w	L	D
10^{-4}	0.15	15	0.23
10^{-4}	0.6	15	0.19*
10^{-3}	0.15	15	2.3
10^{-3}	0.6	15	0.6*

* These figures were derived using a modified relationship between D and θ which takes into consideration the range of values $D \leq w$.

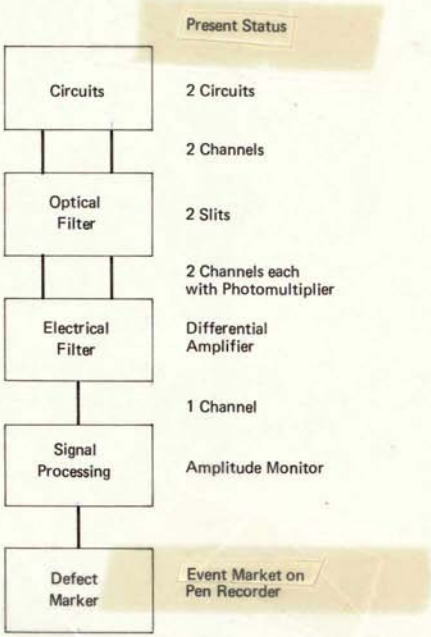

FIGURE 5 A BLOCK DIAGRAM SHOWING THE MAIN FEATURES OF THE INSPECTION SYSTEM

on the figures indicate the current status of the system. Two circuits are inspected simultaneously through two optical spatial filters. The optical signals are converted to electrical signals, subtracted, and processed before an event marker is activated. This is only one of many schemes which can be conceived to implement the same system concept. Only one circuit could be scanned at a time and the information transformed through an optical spatial filter converted to an electrical signal and stored. The electrical filter could consist of a correlation between two stored signals and the signal processing could be a comparison with a decision table before a marker pen is activated to mark the defective circuit. Many of these alternatives are discussed later.

CHAPTER III - THE EXPERIMENTAL EQUIPMENT

The major item of the equipment is a Nikon mask alignment microscope which has two independently adjustable objectives which view two separate circuits on a wafer. By means of a series of prisms and mirrors, the image from one objective or the other can be presented to eyepieces suitable for an observer to use. Alternatively, it can be projected onto one of two image planes, either the film plane in a microscope camera or a ground glass screen suitable for a second observer. Another adjustment allows parts of both fields of view to be seen in the eyepiece or at the projection planes simultaneously. This is the mode of operation used to obtain the differential signals. The camera is removed and a glass mask carrying the two slits is placed at the film plane. One slit covers part of the field of view of one objective while the other slit covers part of the field of view of the other objective. By adjusting the spacing of the objectives, rotating the microscope stage and the skeleton of the camera attachment, the two slits can be aligned on to identical parts of the two circuits. Figure 6 shows schematically the arrangement of the other components and subsystems around the microscope. The various features will be discussed in detail in this chapter.

The scanning action is provided by moving the circuits below the objectives and keeping the slits stationary. Several motors are available with a range of drive speeds for the stage between 5 mil/s and 0.5 mil/s. A simple friction drive was used to drive the stage along the x-axis but later the drive was along the y-axis and then a drive belt was used. The limit on the scanning rate is set by the bandwidth of the electronics in the signal channels, the faster the scan the wider the bandwidth necessary. Unfortunately, this requires more sophisticated electronics and leads to signal to noise problems. If a circuit 100 mil x 100 mil in size is to be inspected in 1 s using a slit 10 mil long so that defects of 0.1 mil in dimension can be detected, then 10 scans are needed, each lasting 0.1 s. Each scan must take at least 1000 samples to an accuracy of a few tenths of a percent so about 10^4 bits of information must be processed every 0.1 s requiring a signal bandwidth of 100 kHz.

Throughout all the experimental work, circuits on wafers were used. The only reason for this was to reduce the difficulties associated with handling chips and aligning the circuits. To a large extent circuits are already aligned on wafers.

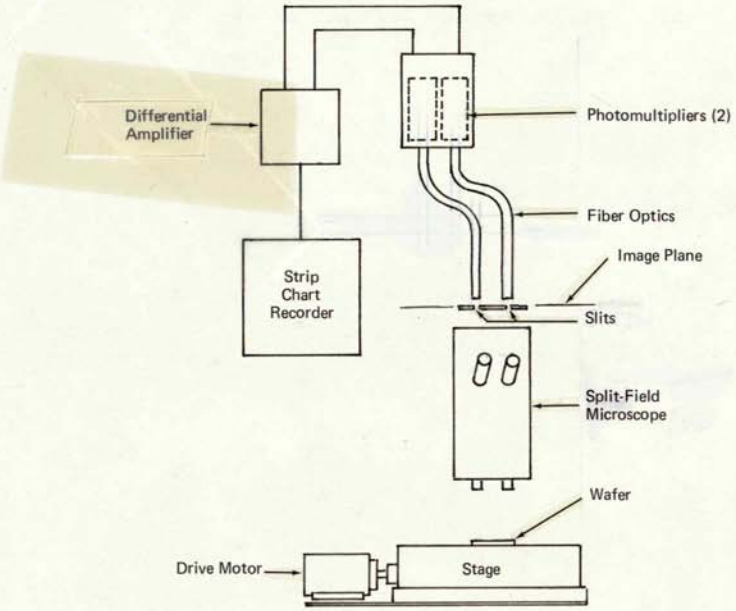

FIGURE 6 SCHEMATIC OF EXPERIMENTAL EQUIPMENT

Because the image is projected onto the camera film plane, the magnification is not readily evaluated from the objectives and eyepieces. However, the measurement of the magnification is straightforward and the various magnification combinations available on the Nikon are given in Table V. The most commonly used magnifications were 27x and 38x. Because slight variations in the throw of the projected image are possible, the real magnification can vary by a few percent from the figures given in the table. The image plane must be parallel to the plane of the mask carrying the two slits. If they are at a slight angle to each other, then one slit sees an image with a slightly different magnification than the image in the other slit. This will lead to measurement noise. The worst case occurs when the image deformation is along the length of the slit. The largest angle between the planes which can be tolerated in this case is 10^{-3} radians.

The illumination system most often used was white light incident normally onto the circuits. This was provided by an 11,000 candle power source. Two fiber optic pick-ups transfer the light to the microscope. There are six illumination levels available at the lamp and an iris in each channel at the microscope. This latter adjustment was not used since altering the iris altered the f-number of the illumination system in an unknown manner, causing unbalance between the channels. A crude adjustment is available to allow the intensities to be equalized in each channel. It consists of a collar supporting both fiber optic pick-ups so that they can be rotated and their position relative to the lamp filament altered. This adjustment was refined a little, but it is still elementary. Table VI gives approximate values of the light intensities at the object and at the slits for several different combinations of light source setting, objective and eyepiece. These measurements are for normal incidence. They were made using a conventional foot-candle meter. The values at the slit plane are only approximate because of the low accuracy of reading the instrument and becaus the reflected light level depends on the circuit being examined. The transmission efficiency of the microscope is in the range 0.1% to 0.5%.

Unfortunately, at the smaller magnifications the constancy of illumination over the field of view is poor when compared to the stringent requirements needed by the inspection scheme. Another unfortunate feature of the microscope, which does not hinder in any way the normal use of the microscope, but which caused difficulties during many experiments in this program, is the spacing between the objectives, which is at least 0.75 in This meant that contiguous circuits could not be scanned and man times there were significant differences between the circuits

TABLE V

MAGNIFICATIONS
(NIKON MASK ALIGNMENT MICROSCOPE)

Eyepiece	Objective	Measured Magnification
4x	5x	13x
4x	10x	27x
4x	15x	38x
10x	5x	32x
10x	10x	64x
10x	15x	96x

TABLE VI

VALUES OF LIGHT INTENSITY AT THE CIRCUIT
AND THE PLANE OF THE SLITS

Illumination at Circuit

Objective	Lamp Setting	Illumination (ft candles)
4x	1	5
	3	14
	5	28
10x	1	2.5
	3	7.25
	5	15

Objective	Eyepiece	Lamp Setting	Illumination(ft candles)
4x	5x	1	0.01
		3	0.025
		5	0.05
4x	10x	1	∿ 0.005
		3	0.015
		5	0.025
10x	5x	1	0.01
		3	0.03
		5	0.07
10x	10x	1	∿ 0.003
		3	0.01
		5	0.02

being inspected. Most notably, the oxide thickness differed in many cases and the difference in reflection coefficients caused an out-of-balance signal masking the defect pulses in the differe tial signal. Preliminary experiments with side lighting were performed but these were not continued when it was observed that the highlights on the metallization occurred at irregular interva and therefore were not the same in each channel. This is a violation of the assumptions listed in Table II. The word "resolution" has been used in two ways during this contract. The normal usage refers to the ability of an image-forming optical instrument to distinguish between two neighboring objects. We have also used this word to describe the smallest feature, whethe it is a defect or a design feature, photometrically observable on a circuit. The image-forming resolution for the microscope is quoted by Nikon in their manual. It is listed in Table VII along with the depth of field. Although typical IC processing does not usually produce variations in altitude over a circuit of more than $\pm$ 5 μm, the smaller values of depth of field which occur at the higher magnifications do appear to cause difficultie during the balancing of the signal intensities in each channel. This is partly due to the sensitivity of the signal to the focusing and partly due to the size of defects, such as foreign particles, which can extend through the depth of field. For these reasons it has been found easier to do most of the experi-ments using the 4x objectives. It is possible to detect smaller objects photometrically than can be resolved in the imaging system.

Considerable experimental work was performed to determine the design of the slits. Neglecting the influence of measurement noise, the best slit appears to be a long thin slit which produce a crisp signature with sharp rise and fall times associated with the passage of each feature across the field of view of the slit. The length of the slit also reduces the number of scans needed to inspect one circuit. The narrower the slit, the greater the band width needed to handle the signals, since the resolution is improved with a narrow slit. As an example a 0.1 mil wide slit scanning across a 100 mil long circuit will take 1,000 separate data points and each data point requires about 10 bits associated with it to accommodate the dynamic range of the gray scale involv so the bandwidth required is about 10kHz in this case.

The need to identify small defects about one slit-width in dimension limits the length of the slit which can be used. If the length of the slit is 100 times the width and the smallest defect is a square which just occupies the slit width, then the maximum area of the slit which it can occupy is 1% of the slit area. Therefore, the largest change in the output signal from the slit caused by the presence of the defect is 1%. This

TABLE VII

RESOLUTION AND DEPTH OF FIELD
OF THE MICROSCOPE

Objective	Eyepiece	Resolution μm	Depth of Field μm
4x	5x	3.0	140
	10x	3.0	90
	15x	3.0	75
10x	5x	1.5	35
	10x	1.5	20
	15x	1.5	17

maximum change in signal only occurs for the maximum contrast defect. Other, lower contrast defects will produce a smaller change in the output signal from the slit. Therefore, the slit length is limited by the need to see some minimum size defect with a specific width of slit.

The analysis of the measurement noise problem, specifically when the noise source is misalignment along the direction of scan, indicates that a short, wide slit is the best to see defects in the presence of misalignment. Therefore, the optimum rectangular slit should have an aspect ratio in the range 20:1 to 100:1. If it is too short, many more scans per circuit are needed; too wide, and the smallest defects are not seen; too long, and the smallest defects are not seen; and too narrow, and misalignment problems are critical.

These comments have assumed a clearly defined rectangular slit. However, by modifying the shape of the slit an improvement in the measurement noise can be achieved. Figure 7 shows some of the various slit configurations tried. The tapered and serrated slits are a partial help in the alignment problem. The transmission at the edges and ends of the slits is reduced by the slit structure, which is an advantage. This advantage is retained as long as the misalignment is less than the depth of the serrations. Otherwise, all that has been done is to delay the onset of the large mismatch when one feature enters the open slit and the same feature is still not in view in the other slit. This delay shows itself as an increased rise time for the pulse. The "shaded" slits show this effect also. On a 0.6 mil wide slit, the serrations take about 0.06 mil on each edge so the basic alignment has to be better than this to take advantage of the serrations. In fact, the figures of Table IV indicate that an alignment much better than this is necessary anyway. Obviously a perfect mechanical alignment is unattainable. With the equipment used it was possible to obtain alignment to about 0.08 mil. The preferred slits are those with the shaded edges or those with the sawtooth edges.

The slits are placed in the image plane so their real dimensions are quite large. However, it is more meaningful to refer to their size in terms of the object dimensions, that is, allowing for the magnification of the system. Typical slit dimensions were 10-20 mil long and 0.15 - 0.6 mil wide. There does not seem to be a single optimum size of slit but experience indicates that these ranges are reasonable.

An obvious alternative spatial filter is a square or circle. No experimental work was done with this type of point scan system because of the following difficulties inherent in the system:

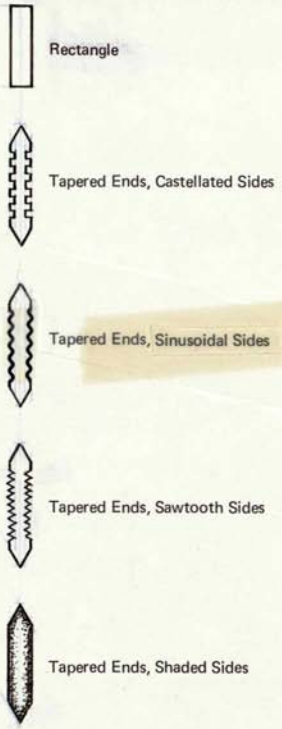

FIGURE 7 EXAMPLES OF SLITS USED DURING EXPERIMENTAL WORK

1. A much larger bandwidth is required; a 0.1 mil square spot inspecting a 100 x 100 mil circuit with a good dynamic range on the gray scale needs about 10MHz bandwidth.

2. The misalignment problems are now critical in two dimensions, instead of one, as in the slit system described here.

3. The spot scan system is much more susceptible to local variations in reflectivity (particularly common on metallization) since it only inspects a small area at a time. The slit tends to smooth these irregularities somewhat by integrating the reflected light over a larger area.

4. The decision criteria must definitely be associated with the use of a computer since it is not clear on any one scan whether an area occupied by a defect filling part of the spot scan is actually only a small defect wholly seen or a small part of a larger defect which must be scanned over many times. The slit scan system offers the possibility of real time decision-making but even if a data store and a computer are used to aid the decision-making, the slit scan requires a smaller data processing capacity.

Although, in principle, the photo-detectors could be placed directly behind the slits, in practice, two fiber optic pick-ups were placed behind the slits to carry the light to the photo-detectors which could then be placed in a more convenient position. The fiber optic pick-ups had a rectangular to round transformation so that they matched well with the slits and the photo-detectors. Two photomultipliers, type 931A, were used to detect the light.

The outputs from the photomultiplier were displayed independently on two channels of a Brush pen recorder. These records are called signatures in this report. The difference signal can then be generated by monitoring the outputs and displaying the signal on one channel of a second Brush recorder. This simple mode of operation was frequently used during the experimental work.

A differential amplifier and amplitude monitoring circuit were built so that the presence of pulses with amplitudes outside a certain range could be detected and displayed on the spare channel on the Brush pen recorder. The circuit built is shown in Figure 8.

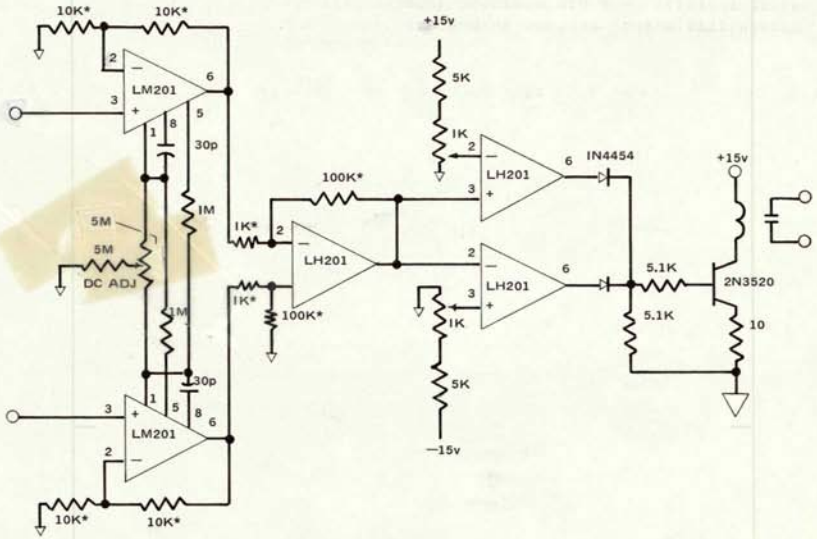

FIGURE 8 CIRCUIT DIAGRAM FOR THE DIFFERENTIAL AMPLIFIER AND AMPLITUDE MONITOR

Figure 9 shows schematically three possible relations between the arrangement of the slits, arrangement of the circuits being scanned and the direction of scan. The configuration shown in Figure 9 (i) was used in the early experiments. However, this configuration is very sensitive to measurement noise generated by misalignments along the direction of scan. One possible way to reduce the influence of the misalignments is to adopt the arrangement in Figure 9 (ii). This certianly reduces the amplitude of the measurement noise but it increases the period of time during the scan when the measurement noise is present (See Chapter II).

This trade-off is not necessarily advantageous. The configuration shown in Figure 9 (iii) was adopted towards the end of the contract since it can be adapted to reduce the influence of measurement noise. The two slits A and B can be made by masking off a single long slit so they are definitely in the same straight line. Then the alignment reduces to a rotational adjustment. The noise caused by misalignment along the length of the slit is not a serious problem. The optimum arrangement would also allow scans of neighboring circuits, but this is not possible with the available microscope.

A few preliminary experiments were performed to establish the feasibility of digitizing the analog data using facilities available at Arthur D. Little, Inc. The experiments were successful but not pursued.

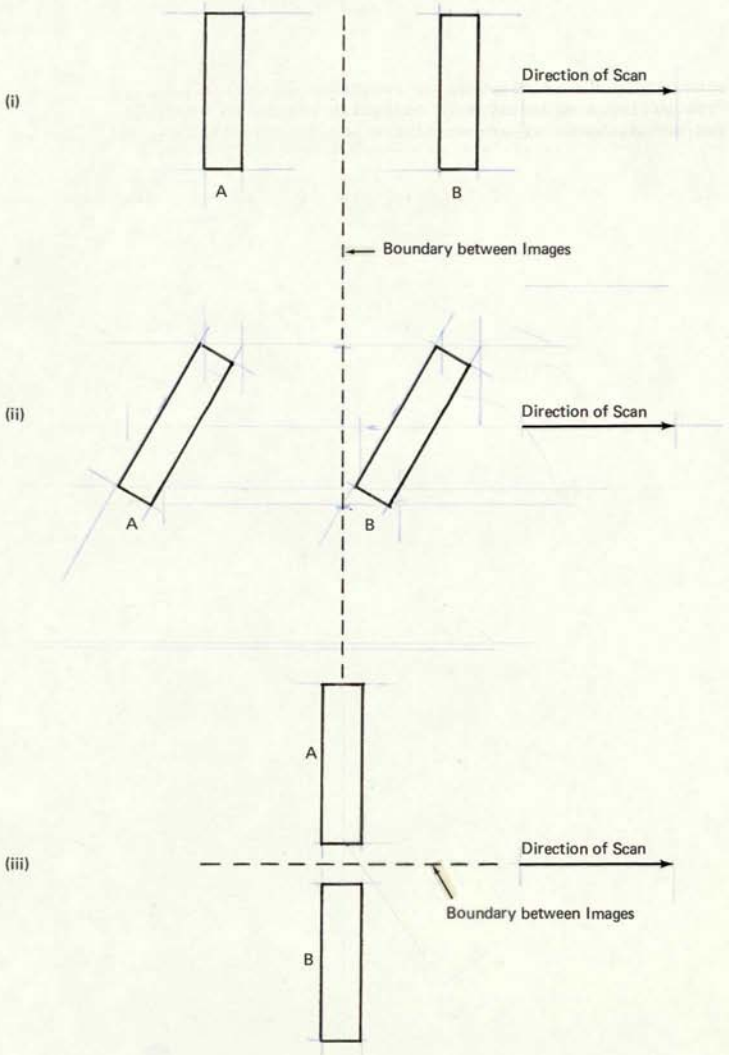

FIGURE 9 THREE POSSIBLE SCANNING CONFIGURATIONS

CHAPTER IV - EXPERIMENTAL RESULTS

Some of the experimental results have already been referred to in Chapter III, in describing the equipment. The main aim in this chapter is to describe the results of the experimental work on the whole system.

Experiments

Photometric Resolution. -- Several series of experiments were performed to examine the influence of the slit size and shape on the photometric resolution. Detailed examination of the signatures produced by scanning a single slit across a circuit led to the following conclusions:

1. The narrower slits reveal more detail, even to the extent of revealing the "noise" detail of the metallization.

2. The rise times associated with the passage of narrow slits over prominent features are much shorter than those associated with the passage of wide slits.

3. The wide slits produce a smoother signature with less detail on it.

4. The tapered, serrated slits do not show obvious differences from rectangular slits.

5. The shaded slits, caused by deliberate defocusing during the photolithographic process, produce signatures with very little fine structure.

The "noise" signal referred to is the signal produced by the polycrystalline structure in the metallization. This is an example of acceptable irregularities in the circuits. There is a trade-off possible between the desire to observe the contributions to the total light reflection made by fine details on the circuit and the desire to avoid the noise contributions to the total light reflection due to the irregular, fine details on the circuits. However, the problems of balance between two signal channels also play a role in deciding the correct slits to use.

Focus. -- Deliberate defocusing of the optical signal produces changes in the signatures but it is difficult to measure these quantitatively. Suffice it to say that a small adjustment of the fine focus does produce a noticeable change.

Perfect Signatures. -- It proved more difficult than expected to produce identical signatures from two or more different perfect circuits. However, it was achieved. The detail of the signature depends on the alignment of the slit and the precision of focusing. It is difficult to make these adjustments from circuit to circuit. The demonstrations of a standard signal were performed by using only one slit and scanning several perfect circuits in sequence. In this way the experimental difficulties were circumvented and it was demonstrated that perfect circuits do produce identical signatures when scanned under constant conditions. Figure 10 shows the photograph of a TTL circuit and below it the signature produced by scanning across this circuit and several of its neighbors. The transparent overlay carries the signature of some of the neighboring circuits and demonstrates that a standard signature for a circuit does exist. The track of the slit is indicated in the figure and several prominent features are noted on the signature. The scribe channels at each edge of the circuit produce prominent and characteristic pulses in the signature. These pulses are so characteristic that they became the standard feature for the experimenter to look for in order to monitor the scans and for the preliminary setting up of the equipment. In fact they are not fiduciary marks, so they cannot be used for precision alignment or signal balancing. The bonding pads at each end of the circuit are clearly visible in the signatures. Note the shoulder on the pulses in the signature where the slit moves over metallization running into the pads. The major run of metallization in the center of the circuit produces a prominent peak also. A more detailed examination of the photograph and chart will show a close correlation between the signature and quite small features on the circuit. Every effort has been made to align the charts with the photographs of the circuits on a one-to-one basis, but this alignment is certainly not perfect in every case. In order to emphasize the features of interest in the other figures in this report, only small portions of a circuit or simple circuits have been used in the examples.

Signatures. -- A lot of useful information was obtained by taking signatures across circuits carefully chosen to show specific features. Figures 11 to 14 show examples of signatures across foreign particles, probe marks, scratches, stains, and missing metallization.

Figure 11 shows a scan across the two end pads of an Apollo gate. A foreign particle, about 1 mil in dimension, is on the right hand pad and its presence is clearly seen in the signature.

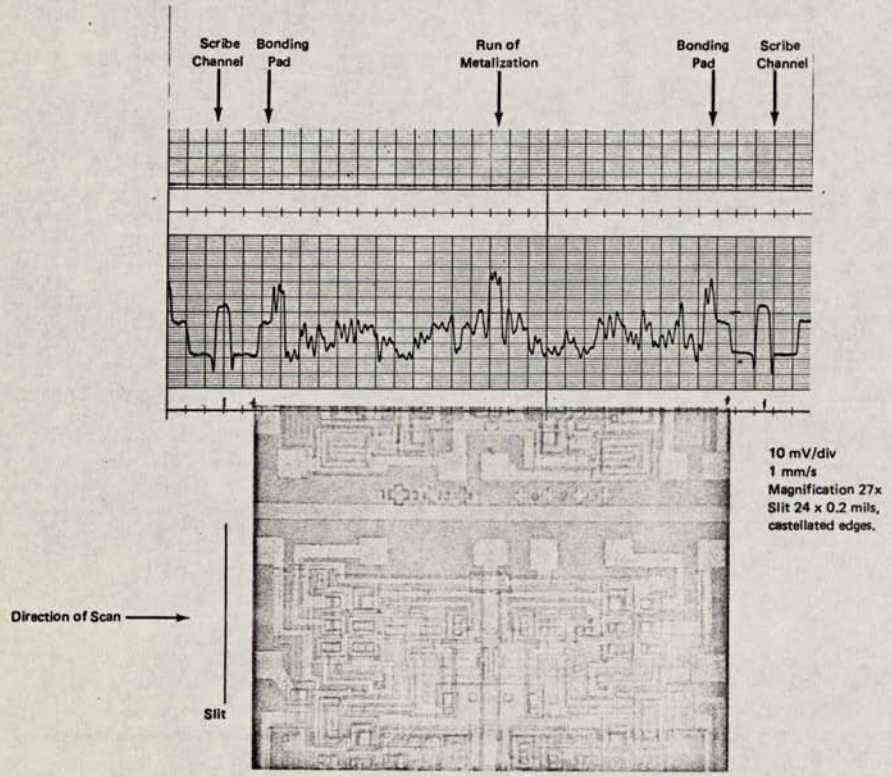

FIGURE 10 STANDARD SIGNATURE OF TTL CIRCUITS

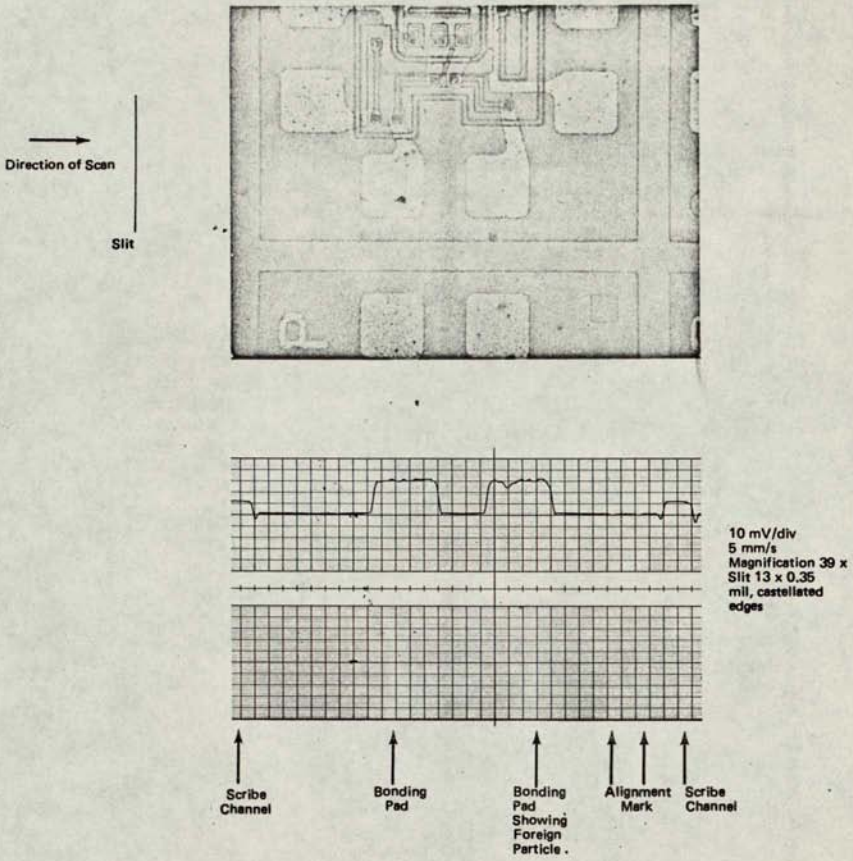

FIGURE 11 FOREIGN PARTICLES ON APOLLO GATE

A second foreign particle close to the scribe channel is not as clearly seen in the signature. This is partly due to the lower contrast of the particle on the oxide compared to the contrast of the particle on the metallization and otherwise due to the 2 or 3 mV ripple on the signature of the pads, caused by the graininess of the metallization. Note that the presence of the low-contrast circular alignment mark is evident in the signature. This is visible because of the quietness of the signal at that point.

Figure 12 is a similar example except this time the defects are scratches on the bonding pads. The major scratch on the right hand pad is about 0.4 mil wide and 6 mil long. Note that the P which is metallized onto the circuit shows clearly in the signature and that the square fiduciary mark at the other side of the circuit is also visible because of the quietness of the signature in that area. It is very difficult to observe the difference in contrast between the mark and the surrounding oxide. The features which are revealed in the signature are the borders to the fiduciary marks.

Figure 13 shows two more foreign particles, the larger being about 1 mil in dimension and the smaller being about 0.3 mil in dimension.

An area of missing metallization can also be seen in the signature of the right hand pad. On the average, this pad produced a signal 4 or 5 mV lower than the other pads. The grainy nature of each pad is clearly seen in the signatures. The pad with missing metal is also distorted and this reveals itself not as a change in signal amplitude but as an increase in the pulse width representing the pad. This can be confirmed by comparing the pulse widths for both pads.

Figure 14 shows a signature of an Apollo gate including probe marks on pads, foreign particles on the scribe channel, and a large stain on the oxide. The larger probe mark is about 3 mil by 2 mil, while the smaller probe mark is about 2 mil by 1 mil. The stain on the oxide is at least 10 mil in dimension. The probe marks are clearly seen in the signature of the pads and the stain is recognizable, since it reduces the signal level to 10-15 mV below the normal level for the oxide revealed in the region between the pads.

These photographs and charts only represent examples of signatures taken on circuits. Many more were taken with the objective of gathering data on the smallest size of defect which could be seen in each class and which parameter is the best to characterize the defect. The approach adopted was to examine closely the signatures of many defects and calculate the amplitude, pulse width, and integrated area of the defect pulse which would be formed if a perfect signature was subtracted from the first signature. Then these parameters were plotted as functions of

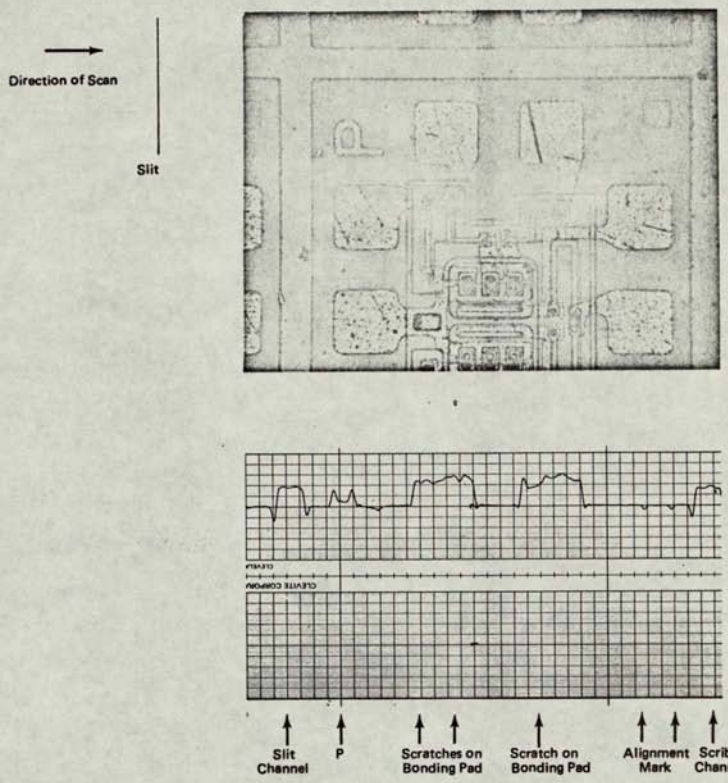

FIGURE 12 SCRATCHES IN METALIZATION ON AN APOLLO GATE

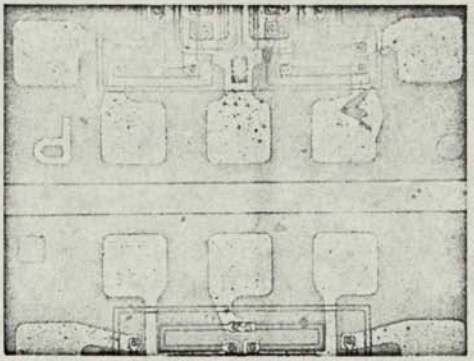

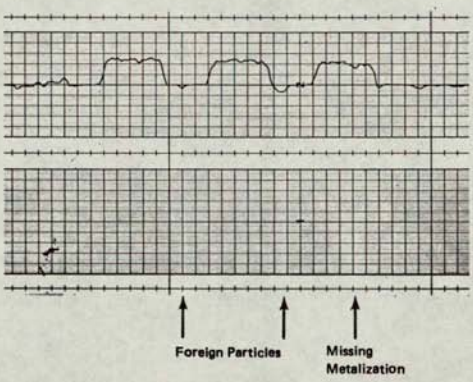

10 mV/div
5 mm/s
Magnification 39 x
Slit 13 x 0.35 mil,
castellated edges.

FIGURE 13 MISSING METALIZATION AND FOREIGN PARTICLES ON AN APOLLO GATE

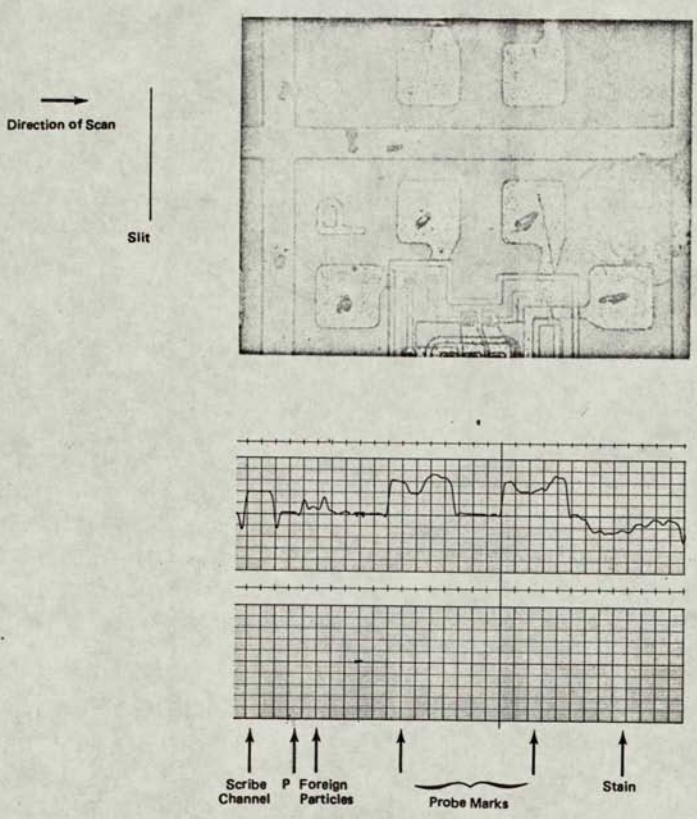

FIGURE 14 PROBE MARKS A STAIN AND FOREIGN PARTICLES ON AN APOLLO GATE

various parameters of the defect, such as its length, width and area. Figures 15 to 19 show typical results obtained. Figures 15, 16 and 17 are graphs for black foreign particles on oxide. As can be seen there is considerable scatter in the results, mainly because of the difficulty of making a quantitative estimate of the contrast for each defect. Figure 15 relates the length of the pulse to the length of the particle along the direction scan. The straight line is a theoretical prediction for a scanning speed of 0.36 mils/s. In Figure 16, the peak voltage of the defect pulse is plotted as a function of the length of the defect along the slit. In this case the straight line is not based on a theory but indicates the trend of the results. Figure 17 relates the integrated value of the defect signal to the area of the defect. Again the line shows a general trend not a theory. Figures 18 and 19 show the relationship between peak voltage and length of the defect along the slit for the case of probe marks and scratches on the metallization.

In the inspection experiments using the differential scheme the parameter which was monitored was the peak amplitude of the defect pulse. This is related to the length of the defect along the slit and the results in the graphs indicate that, in order to detect black foreign particles on the oxide or scratches, in either case extending less than 1 mil in length along the slit, the system must be sensitive to 2 mV pulses in the differential output. Probe marks on the metal pad must have a higher contrast because to detect them at 1 mil size needs a sensitivity of only about 5 mV.

Table VIII gives a list of the smallest defects which can reasonably be detected in a signature by an experienced observer. Care must be taken in interpreting these figures, since they represent minimum values associated with the maximum contrast. Lower contrast defects will have larger minimum sizes. Also, the minimum size in many cases is dictated by the fact that smaller examples of the defect were not available on the circuits used in the experiments. An obvious example of this is the value for probe marks. The dimension given represents the critical dimension in each case, the width of a scratch and the diameter of a foreign particle, for instance. Reliable experimental data for some types of defects is still not available, either because the defects were never seen or because they were only seen in ambiguous circumstances.

Differential Signals. -- The major aim of the contract is to demonstrate the feasibility of an automated visual inspection system for integrated circuits. An operator detecting defects in the pen recording of a signature is certainly not detecting defects automatically. Many experiments were performed to test the efficiency of the automated scheme, using a differential amplifier for the electrical filter and a threshold monitor for the GO/NO GO decision.

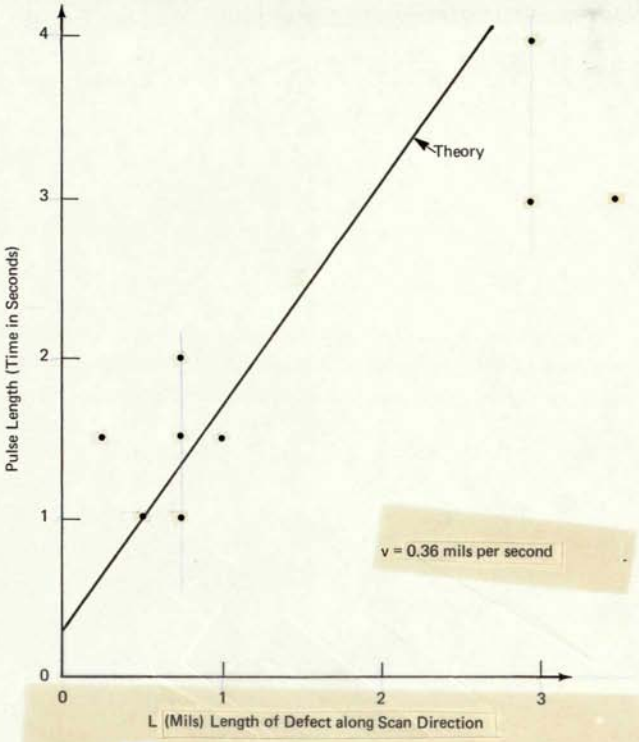

FIGURE 15 BLACK FOREIGN PARTICLES ON OXIDE
(Pulse Length Versus Length of Defect along Scan Direction)

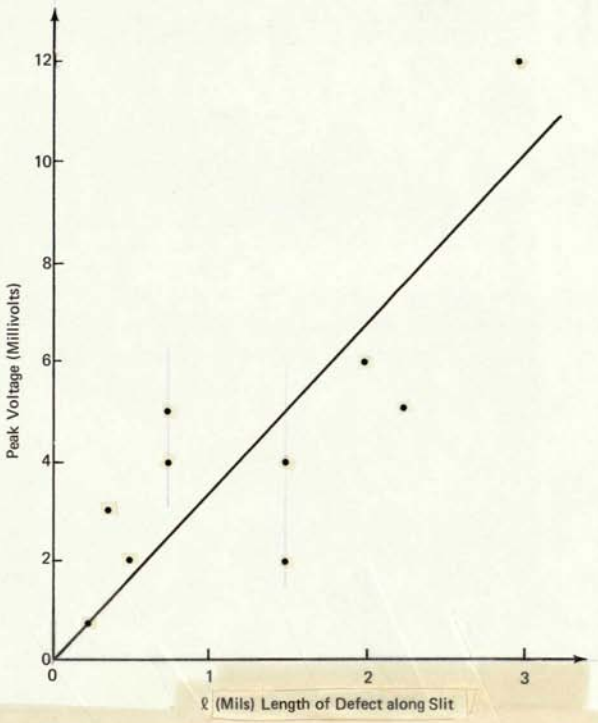

FIGURE 16 **BLACK FOREIGN PARTICLES ON OXIDE**
(Peak Voltage Versus Length of Defect along Slit)

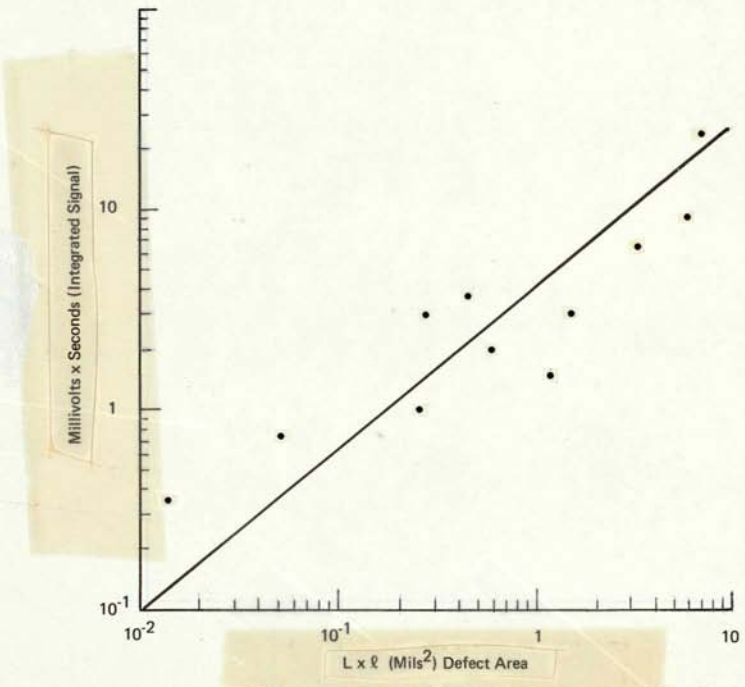

FIGURE 17 BLACK FOREIGN PARTICLES ON OXIDE
(Integrated Signal Versus Defect Area)

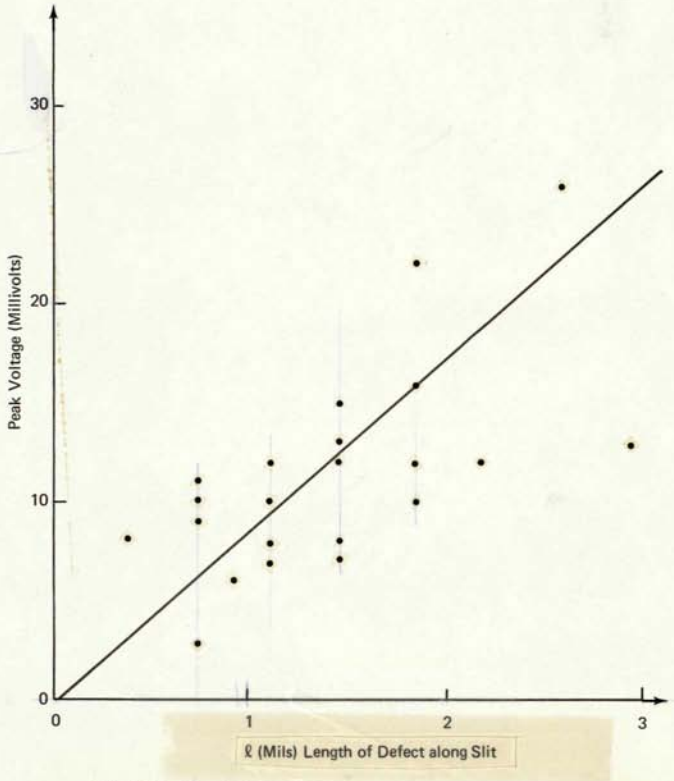

FIGURE 18 PROBE MARKS
(Peak Voltage Versus Length of Defect along Slit)

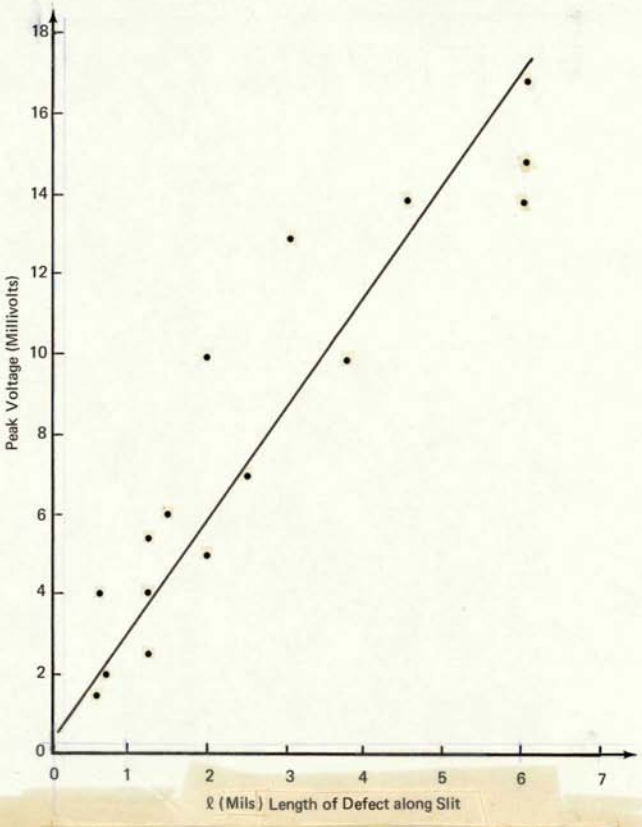

FIGURE 19 SCRATCHES ON METALLIZATION
(Peak Voltage Versus Length of Defect along Slit)

TABLE VIII

DEFECTS OBSERVED IN SIGNATURES

Type	*Size (mil)
Foreign Particles	0.1
Scratches on metal	0.1
Extra metal	0.2
Missing metal	0.2
Probe marks	0.4
Oxide discoloration	0.7
Missing diffusion	1
Corrosion	2
Ink blotches	5
Contact window	∿.1

Maximum contrast defects quoted.

*Principle dimension

Figure 20 is an example of a scan across two Apollo gates, one with a 4 mil diameter foreign particle on a pad and the other with a 1.5 mil wide scratch across the neck of a pad. The two signatures and the differential signal are shown. Note that the chart recording of the differential is at 5 mV/division while the recordings for the signatures are at 10 mV/division. Also, the scan cannot be shown on the photographs because the circuits had to be moved in order to take the photographs. Basically, the slits crossed the first of the side pads, then part of the active area, and moved out over the directly opposite side pad. They did not cross the end pads but they crossed the metallization neck on the end pads.

It is more difficult to associate the differential signal with features on the circuits than it is for the signatures. The threshold monitor was not operating during this scan so it is necessary to fix limits on the chart. Thresholds at $\pm$ 15mV are indicated at the left side of the differential chart. Inspection of the chart shows that two pulses cross that level, one related to the presence of the foreign particle on the pad and the other related to the scratch on the metallization. The different signs of these defect pulses are related to the fact that they are both dark defects on metal but in different channels.

As pointed out above in the discussion of Figures 15 to 19, in order to detect small defects it is necessary to be able to detect defect pulses of 1 or 2 mV.

Therefore, the choice of $\pm$ 15mV for the thresholds is obviously inappropriate in a working system. If the thresholds are dropped to $\pm$ 10 mV, then the scribe channels give defect signals. In fact, throughout all the experimentation it was very difficult to avoid false alarms from the scribe channels. This is mainly because they are not fiduciary marks on the circuit. Reducing the threshold to less than $\pm$ 8 mV gives false alarms associated with other features on the circuits. Almost certainly this is due to out-of-balance signals between the channels. This in turn is probably due to mechanical misalignments and to differences in illumination intensity between the channels. With the apparatus used for the experimental work it was difficult to align to better than 50 µin; 80 µin is probably a more realistic figure. When this is compared with the estimates in Chapter II it is easy to see why the differential signal is so noisy. The illuminator associated with the microscope is also not adequate for the task demanded of it and out-of-balance signals associated with the illumination of about 0.5 mV were typical. Another feature of many of the differential traces taken was the marked difference in the color of the oxide. This is a permanent bias in the differential signal, which means that setting the amplitude monitor is not a reliable way of detecting defect pulses.

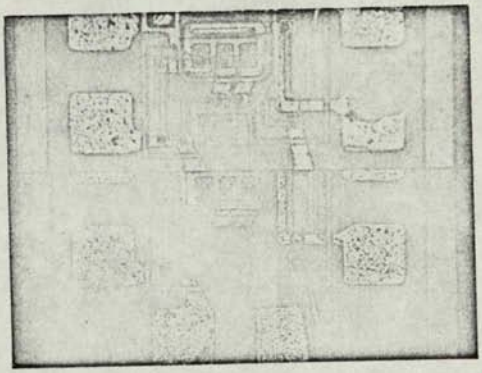

Direction of Scan

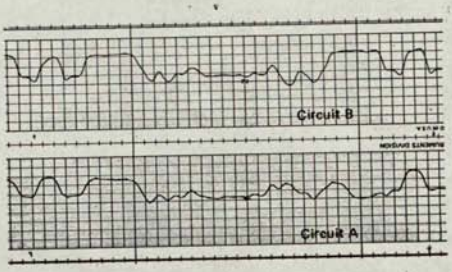

Signatures 10 mV/div
Differential 5 mV/div
5 mm/s
Slit 13 x 0.35 mil
Castellated edges

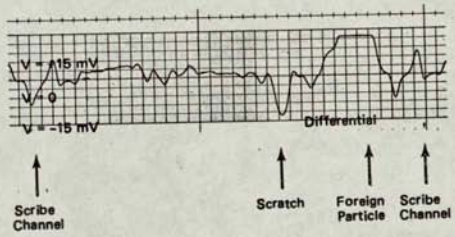

FIGURE 20 EXAMPLE OF A DIFFERENTIAL SIGNAL

Figure 21 shows the signatures of two similar scans across two Apollo gate circuits with the differential signal on the third channel and an event marker on the fourth channel. The marker was set to operate at $\pm$ 8 mV. The two probe marks were detected by the system and the event marker was activated. The passage of the scribe channels under the slits also activated the event marker on the negative going excursion only. This indicates that the 16 mV window was probably not symmetrically arrayed about the zero level.

Table IX summarizes the results of many experiments. As in the case of Table VIII, the figures for the minimum defects are not absolute minima but reflect what has been seen. The figures are for maximum contrast defects. Lower contrast defects are more difficult to see.

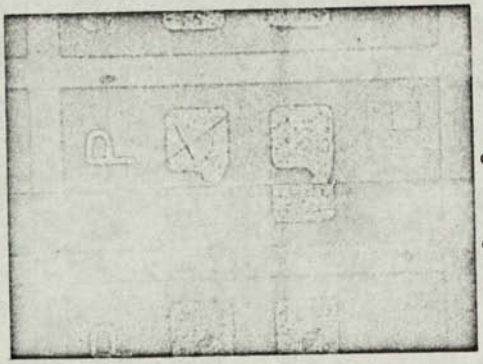

Direction of Scan

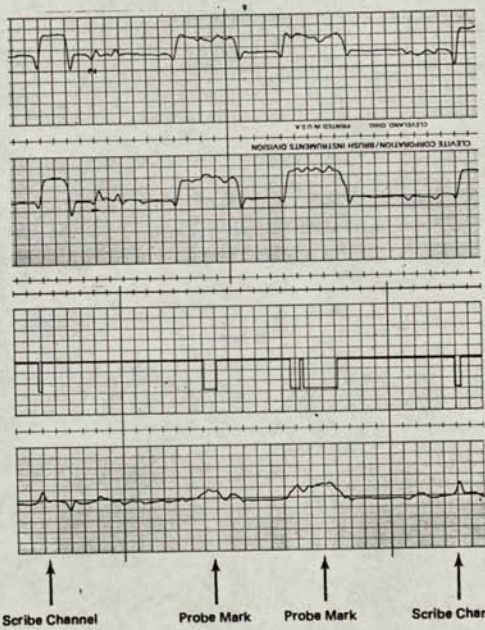

Signatures 10 mV/div
Differential 10 mV/div
Event marker IV/div
5 mm/s
Slit 13 x 0.35 mil
castellated edges
Amplitude monitor
± 8 m V

FIGURE 21 DIFFERENTIAL SIGNAL SHOWING EVENT MARKER

TABLE IX

DEFECTS OBSERVED IN DIFFERENTIAL SIGNALS

Type	*Size(mil)
Foreign particles	1
Scratch in metal	1
Probe marks	1
Missing diffusion	1
Oxide disoloration	1
Ink blotches	5

Maximum contrast defects quoted.

*Principle dimension

CHAPTER V - DISCUSSION

After extensive experimental work the following conclusions can be drawn:

1. Defects on integrated circuits have been detected automatically, using a system with mixed optical and electrical signal processing.

2. The optical specifications of such a system have been investigated in detail and the most important parameters established.

3. The electrical specifications are not so clearly established, especially those for the decision making process.

4. Little work was done on the mechanical handling of circuits but it was possible to establish clearly the alignment tolerances to be placed on the circuit handling equipment.

5. The minimum size of defect seen was limited by the performance of the equipment rather than by the inspection technique. At present, the minimum size of defect detected in the differential signal is too large to find an immediate widespread application.

6. The minimum size of defect observable by an experienced observer in a signature is much more compatible with NASA's and industry's requirements. This indicates that further work needs to be done on the electrical filtering and signal processing to utilize more completely the information in the signatures.

7. There is reasonable agreement between theory and experiment, especially in predicting the limits set on observable defect size by measurement noise.

8. The results of the demonstration carried out at the end of the project indicate that about 5% of the defects on a set of circuits can be detected. It is difficult to establish firm statistics, particularly a definite level of confidence. For large, high contrast defects (e.g., a black foreign particle on metal with a diameter of 2 mil), the chance of detecting the defect is close to 100%, but for a lower contrast

defect or a smaller defect (e.g., a black foreign particle of 1 mil diameter on oxide) the confidence level for detecting the defect has dropped to a few percent. Table X contains a more detailed breakdown of the results of the demonstration.

9. The specific limitations on the experimental apparatus were:

   a. mechanical alignment of the circuits under the slits;

   b. differences in focus between the objectives;

   c. non-uniformity in illumination between the slits and along each slit; and

   d. the impossibility of scanning near neighbor circuits.

Discussion of Improvements

Having established the basic feasibility of the inspection scheme suggested, the main question now is "How can we improve it?" A large number of possible improvements and alternatives have been studied. Only the main ones will be reviewed here. Choosing from many of these ideas depends on several criteria, besides the ability to detect small defects reliably. Particularly, it depends on such things as the user's preference for a self-contained machine or an operator's aid, whether the user is prepared to dedicate data processing time to the system on an existing facility or whether he needs the data handling equipment included, and on whether the user demands real time operation or is prepared to wait, perhaps only a few minutes, for the results of a scan. Another important feature is the availability of diagnostic features on the equipment. In general, it has been assumed that a simple real-time system with the ability to make GO/NO GO decisions about circuits on wafers is the most desirable machine. Since the system concept contains several subsystems (See Figure 5), it is possible to take several of the ideas to be discussed here and interchange various subsystems to make up new systems. We have noted in this chapter where significant improvements are likely to result.

The possible alternatives will be discussed under the next three headings.

TABLE X

CIRCUITS SCANNED DURING
THE DEMONSTRATION

Type	Total Number of Defects Seen in Preliminary Visual Inspection		Total Number of Defects Seen in Differential Signal	
72 unmetallized Signetics circuits	D	36	D	9
	FP	∿400	FP	15
	PH	8	MD	2
	MD	3	Defects in dielectric	1
	ED	1		
	Defects in dielectric	1		
58 metallized Signetics circuits. 18 only 50% coverage	D	∿25	D	4
	FP	∿100	Sc	1
	Sc	5		
	Poor metal	6		
	PH	several		
32 metallized Apollo gates, only 50% coverage	FP	∿100	FP	1
	Sc	∿25	Sc	1

In all cases, the oxide thickness shows distinct changes across the wafers, tending to dominate the differential signal.

ABBREVIATIONS:

D	Discoloration
ED	Extra diffusion
EM	Extra metal
FP	Foreign particle
MD	Missing diffusion
MM	Missing metal
PH	Pin hole
S	Scattered
Sc	Scratch

Direct Approach. -- The first thought is to attack the problem directly and improve every feature. The system should have the capability of inspecting nearest neighbor circuits. It needs 40x or 60x magnification; the upper limit is set by the desire to scan a reasonable track across a circuit and by the limitations on the depth of field. The illumination must be constant over both fields of view to better than 1% and the adjustment in intensity between the channels must not spoil this constancy. Achieving this accuracy of control over the illumination is quite complex. The optics of the illumination system must be well-designed. It will certainly be necessary to use a diffuser and a graded density neutral filter in the illumination channels. In order to avoid highlight effects the light must be incident on the circuits very closely to the vertical. The focus in the two channels must be identical. This implies a flat wafer on a horizontal stage without curvature of the field of view. It is best to gang the focusing of the two objectives. An automatic focusing feature could be used if each circuit carried a fiduciary mark for the purpose. Since one of the recommendations to aid the alignment is that each circuit carry a fiduciary mark, this is no difficulty. The alignment should be to better than 10μin.

Automated focusing and alignment attachments are being built for step and repeat cameras, mask alignment systems, etc. One elegant system is based on two comb structures which are moved past each other and modulate the amplitude of a light beam. Alternatively, a laser interferometer system could be used. The best way to operate would be to have the stage stop at the beginning of each circuit while checking the circuit alignment and focus. However, if the depth of field of the objectives and the tracking of the stage are adequate, one setting per scan across the wafer should be adequate. Since more than one scan across each circuit will be necessary for 100% coverage, the fiduciary marks must be repeated at different positions on the circuits. This is necessary in any case for the mask alignment stages of wafer processing.

The illumination intensity must be balanced between the channels and this is best done against some standard reflecting surface which is inserted at the appropriate moment in the optical system. The motion of the stage need not necessarily be uniform as long as each circuit moves under each objective in synchronism. For increased confidence the photomultipliers and the differential amplifier need stabilized power supplies. Since the scribe channels are going to give false alarms in the differential channel, a clock is needed to indicate the time window during which the scribe channels are passing beneath the objectives. With all these improvements the system is likely to be able to detect high contrast defects down to a few tenths of a mil.

A modification of this scheme which might be applied at low magnifications, say 20x, is to use only one objective but with such a large field of view that two circuits are viewed side by side. Then, there is no need to worry about differential adjustment between the optical channels. The alignment becomes more a question of rotation than anything else. There is, however, a special requirement on the slits that they now need to be adjustable with respect to each other. Also, this concept puts especially stringent requirements on the illumination over the field of view. A large field of view and constant illumination over the whole field of view do not normally go together. This approach was in fact tried and was unsuccessful because of the illumination problems on the available equipment.

Multi-segment Slits. -- Although, in Chapter III only one relation,

$$\frac{S}{N} = \frac{Dw\Delta R}{L\Delta wR},$$

was given for the measurement noise, this in fact is a special case for the situation when the dimension of the smallest size defect is larger than the slit width. If this is not the case, then

$$\frac{S}{N} = \frac{D^2\Delta R}{L\Delta wR}$$

for a square defect. In each case, the length of the slit plays a significant part in determining the minimum size defect. By utilizing a coherent fiber optic pick-up behind the slit which does not transform to one circular output but to many, say ten, outputs, it is possible to make each slit behave like ten short segments. The signals from each segment would be treated separately, so ten photomultipliers are required for each channel.

The improvement in the measurement noise situation is shown in Table XI for segments of varying lengths and for various misalignments. Obviously, detecting a defect in one segment means a rejected circuit, but it is also necessary to compare the differential signals associated with pairs of neighboring segments since, in the worst case, a definite defect, 0.1 mil long, may be halved by the segments to look like two acceptable deviations from the circuit features, each 0.05 mil long. The obvious disadvantages are: the increase in the amount of electronics; the need to balance many photomultipliers; and the cost of the fiber-optics. The major advantage is the reduction in measurement noise. This approach has advantages over a point scan since it consists of several quite large point scans simultaneously and is therefore faster.

TABLE XI

MEASUREMENT NOISE IN MULTI-SEGMENT SLITS

$\frac{S}{N} = nD^2/L\Delta w$,

$\frac{S}{N}$ is the signal to noise ratio,

n is the number of segments forming the slit,

D is the side length of a square defect,

L is the length of the slit,

Δw is the misalignment along the direction of scan.

Assumptions

$\frac{S}{N} = 3$,

L = 15 mil,

D < w, the width of the slit,

The misaligned feature has the same contrast as the defect,

All dimensions in mil.

Δw	n	D
5×10^{-3}	10	1.5×10^{-1}
10^{-2}	10	2×10^{-1}
2×10^{-2}	10	3×10^{-1}
2×10^{-2}	20	2×10^{-1}

Two-dimensional Optical Filtering. -- Although the optical filters based on rectangular slits are very effective in suppressing the information from circuit features with major dimensions along the direction of scan, the same slits actually enhance the presence of the circuit features with major dimensions along the slit. The enhancement of slight misalignments between these features is the main source of measurement noise. The multi-segment slit is one possible way of overcoming this but an alternative technique is to scan another set of slits along the major slit (See Figure 22.).

The analysis of this filtering technique is most obvious if it is assumed that the secondary slits scan completely across the primary slit while it is covering the same field of view. If the system is to scan a 100 mil circuit in 1 s this implies a scan rate of 0.1 in s^{-1} for the primary slit. If a second requirement is resolution to 0.1 mil, then the primary slit views the resolution element for 1 ms. Assume that the primary slit moves in a stepping motion, advancing in an infinitesimally short time and stopping for 1 ms before advancing again. In this situation the secondary slits must scan from end to end of the primary slit in 1 ms; if the primary slit is 15 mil long this is 15 in s^{-1}, which is not an unrealistic velocity requirement. It is better to use multiple secondary slits because of the overall intensity requirements. A single secondary slit of width equal to the width of the primary slit reduces the area for transmission of light by about 100x. Using multiple secondary slits with a mark to space ratio of 1:1, the light intensity is reduced by 2x only. In this case, there is little need to worry about noise in the response of the photo-detector. Also, the multi-slit arrangement gives rise to a repetitive signal from the features viewed, rather than to a single shot signal.

The advantages of this arrangement can be seen by reviewing the measurement noise from a misalignment along the direction of the primary scan. For convenience in all the calculation, it is assumed that the defect contrast and the reflectivity of the misaligned feature are equal, and that a signal to noise ratio of 3 is acceptable. Operating at a signal to noise level of 1 is not reliable, since there will be electrical noise pulses causing false alarms. Therefore, to increase the reliability, a signal to noise ratio greater than 1 is necessary. If the defect is a square with dimension smaller than the slit width it will be modulated entirely; at one position of the secondary scan it will all be obscured while at another position it will all be in view. Misalignment in the worst case occurs when a long feature moves into the view of the primary slit. If this feature extends the whole length of the primary slit, its signal will not be modulated by the secondary slit (assuming an equal number of opaque and transparent regions in the secondary slit). If the misaligned feature does not extend the whole length of the primary slit, it also produces a modulated signal, but of an amplitude limited by the width of the secondary slits. The worst case occurs if the

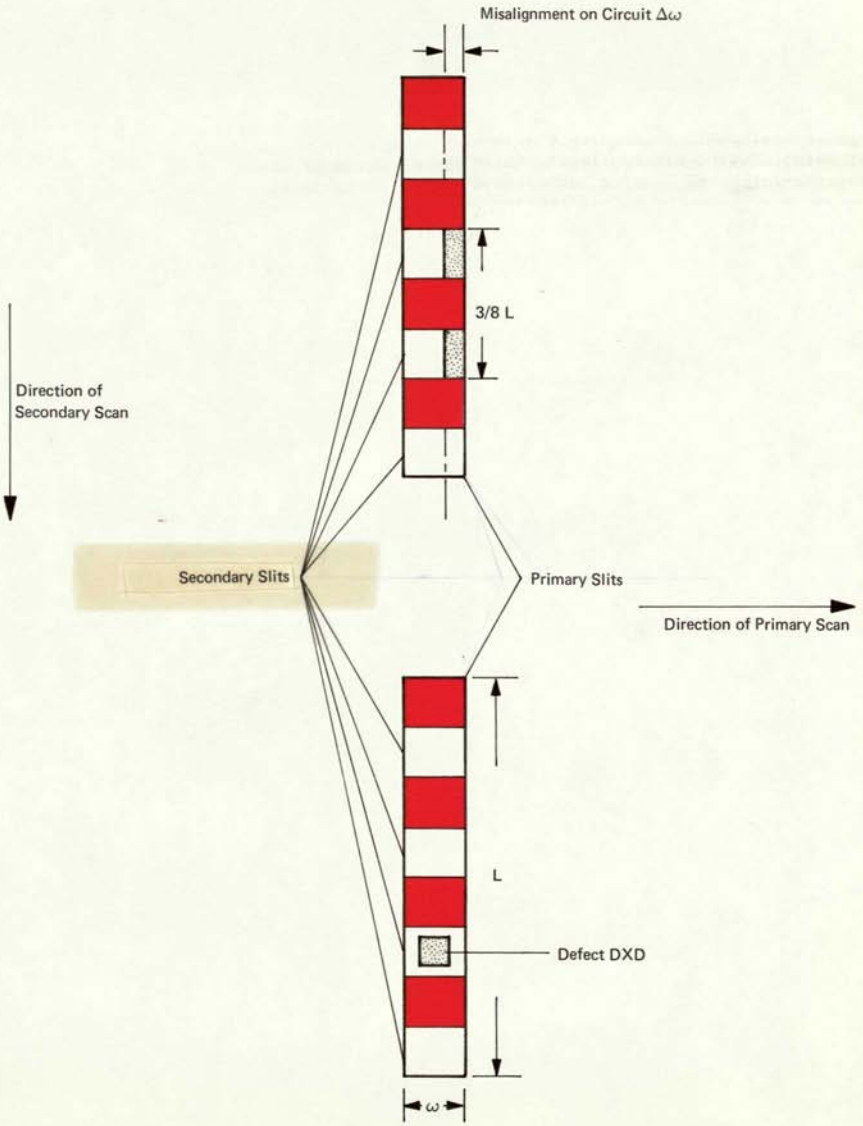

FIGURE 22 SCHEMATIC OF TWO–DIMENSIONAL SCAN SCHEME

misaligned feature is an odd integer number of slit widths long, say 3, then the signal is modulated from 2 sections visible to 1 section visible, etc., by the passage of the secondary slits. If the defect is an even number of slit widths long it is not modulated. Table XII shows some theoretical predictions for the minimum size square defect based on the situation shown in Figure 22. As can be seen, there is some improvement over the multi-segment case and the more elementary single slit case. This improvement has been gained at the expense of a more complex scanning arrangement and a wider bandwidth for the system. However, it has the advantage over the multi-segment case of not needing a multitude of detectors and multiple signal processing channels. In order to detect reliably 0.1 mil features in a 1 ms scan along a 15 mil track with a reasonable grey scale, it is necessary to provide a 1.5 MHz bandwidth. It is not feasible to use a synchronous processing signal because of the great variety of wave forms which the system will generate.

There must be precise synchronism between the secondary scans over the two slits or there will be further alignment problems associated with the signals entering the differential amplifier. It has proved difficult enough to get alignment between two signals with a few Hz bandwidth, let alone signals with about 1.5 MHz bandwidth.

Electrical Filtering. -- In principle the existing optical filtering provides adequate information in the signatures. The problems were associated with synchronizing the information from two channels and performing suitable electrical filtering on the signal. Many different electrical filtering procedures have been considered. Some are reviewed here.

Integrate the Signals. -- A typical small defect is assumed to be 0.25 mils long on a 50 mil chip. The output signal from such a defect is about 1 mV.

The integral method requires the comparison of the unknown signal with the area under the curve of a standard signal. Now:

$$A_{standard} = \int_{V}^{T} dt = \langle V \rangle T,$$

and

$$A_{defect} = A_{st} \pm k\Delta V \Delta t,$$

where k depends on the shape of the defect.

TABLE XII

MEASUREMENT NOISE WITH TWO-DIMENSIONAL SCAN

$\frac{S}{N} = nD^2/L\Delta w$,

$\frac{S}{N}$ is the signal to noise ratio,

n is the number of secondary slits,

D is the side length of a square defect,

L is the length of the primary slit,

Δw is the misalignment along the direction of scan.

Assumptions

$\frac{S}{N} = 3$,

L = 15 mil,

D < w, the width of the slit,

$n = \frac{L}{2w} = 25$ (w = 0.3),

The misaligned feature fills an even number of secondary slits and has the same contrast as the defect,

All dimensions in mil.

Δw	D
5×10^{-3}	10^{-1}
10^{-2}	1.4×10^{-1}
2×10^{-2}	1.9×10^{-1}

Therefore, the system must be capable of detecting changes in the value of the integral of

$$\pm \frac{k\Delta V\Delta t}{\langle V\rangle T} \times 100\%$$

To a good approximation:

$$\Delta t/T = 2.5 \times 10^{-1}/5 \times 10 = 5 \times 10^{-3},$$

$$\Delta V/\langle V\rangle = 5 \times 10^{-2},$$

and $K < 1$, typically 1/2.

Therefore:
$$\frac{k\Delta V\Delta t}{\langle V\rangle T} = 125 \times 10^{-6}.$$

That is, the system must be capable of detecting changes in the integral of about 1 part in 10^4.

There are two main sources of error (other than instrumentation error during the integration). These are acceptable deviations between circuits, particularly in reflection coefficient, and integration over the wrong window of the signature.

Variations in reflection coefficient are most obvious on the metallization and could quite well make a contribution of $k\Delta V\Delta t$ to the signal. On the Apollo gates metal crystallites of a similar size to the assumed defect have been seen. It is fairly simple to maintain the same integration time but it is essential to start the integration at the same place on each circuit. If there is a good oxide "frame" round the circuits, there is a slight relaxation of this condition.

Take the Perimeter of the Envelope. -- This idea suffers from the same defects as that above; namely, detecting a small variation in the length of the envelope in the presence of variations in reflection coefficient and slight misalignment of the sampling system. This system is also critically dependent on the slope of the various parts of the signature since small variations in slope due to passage over an ill-defined edge to a feature cause changes in the periphery, especially when the feature gives rise to a marked peak.

Counting Zeros. -- This seems entirely inappropriate. A defect may cause a slight deviation at one extreme or the other of the signature and not introduce an extra zero crossing at all.

Counting maxima and minima. -- This requires differentiation of the signal and a pulse count into a register whenever the signal passes through a maximum and another pulse count into a register when it passes through a minimum.

Since a defect on the side of a steep slope may only cause a point of inflection it will also be necessary to count these. This could be done in analog format or perhaps better in digital format. It would be necessary to consider groups of data points rather than individual samples. A defect would be detected by the presence of different totals in the three registers between scans. Metallization noise may be a problem here. Consideration must be given to the correlation between defects found and defects missed. Attempts to do this by examination of chart records have not succeeded.

Transforms. -- It is difficult to say what the efficiency of a Fourier transform (or something similar) in detecting defects would be. However, the philosophy of this contract has been to establish a real-time system. A transform system requires extensive calculation. Even a fast-Fourier transform using the Tookey algorithm requires 30-60 seconds of processing time for a relatively simple case. A slight, constant delay between scan and processing would be acceptable but not the delay associated with a Fourier transform.

Correlation. -- This suffers from all the defects of the transform scheme. The process time required varies as N^2 where N is the number of data points taken. This system seems to be prohibitively expensive in computing power.

Digital Techniques. -- Any of the electrical filtering techniques discussed above can be digitized and the signal processing done in the digital domain. This allows more sophisticated decision criteria to be applied, since a signal can now be subdivided cleanly into section both by time and by amplitude. Then particular features can be identified in terms of their occurrence in these sections. This adds some diagnostic capability to the signal processing.

Some preliminary experiments were performed to establish the compatibility of the inspection gear with a data acquisition facility available at Arthur D. Little, Inc. The experiments were successful but no further signal processing was performed. The system took data from scans across circuits made at about 1 minute per scan and digitized at 60 samples per second with 12-bit resolution. The basic system can operate at 20,000 samples a second which is adequate for single slit scans across a circuit in a few seconds. To accommodate the data rate associated with the two-dimensional scan system, a sampling rate of about 2 MHz is necessary. The 12-bit resolution was used because it was available. Experience shows that signals of 50 mV amplitude are produced by the scans, and since about 0.2 mV resolution is required to detect small defects, an 8-bit resolution is probably acceptable.

Although analog and digital signal processing can be done both in real time and on stored data, there is most advantage to be gained from storing the digitized data and doing processing at a later time. One of the immediate possibilities is that of performing trial realignments of the data to remove any residual measurement noise. In fact, many of the alignment problems can be removed from the experimental domain completely by using just one scanning system and doing the electrical signal processing on the data from consecutive circuits.

A suitable storage mechanism for this type of system would be a disk drive carrying a disk with several tracks. The data from one signature is stored on one track and the whole unit has a rotational time equal to the scan time so that the next signature goes onto the next track starting in the same sector. Alignment of the digital data is made easier by placing fiduciary marks on the circuits.

The multi-segment scan requires several analog to digital converters in parallel. The number can be reduced somewhat by multiplexing between the photomultipliers and the converters.

Many different systems and subsystems have been described. The one which places the least requirements on the alignment and balance procedures is a combination of a single channel with digital data processing and counting of maxima and minima. However, a preliminary evaluation shows that this technique does not necessarily combine high reliability and high resolution.

The two-dimensional scan and the multi-segment scan both offer reduced measurement noise in return for more complex scanning systems. The alignment problems associated with the simple scanning system indicate that it does not offer sufficient resolution to make a practical system. The translational and rotational alignment problems, the focus, and the uniformity of illumination can all be adjusted to a reasonable minimum but the ultimate limitation of all systems is the presence of acceptable deviations between circuits, especially changes in reflection coefficient from point to point on the metallization.

Aids to an Operator. -- There are several ways in which the system could be adapted to aid an operator. The most simple would be to have the machine stop the scan whenever the threshold monitor detects an excursion over a certain voltage and tell the operator where and on which circuit to look for a possible defect. Another possible mode of operation is to give the operator a transparency of the chart of a perfect circuit to place over the charts being produced during the inspection and check for deviations visually. A modification of this would be to put the scans on a storage oscilloscope and compare with a suitable transparency. These techniques rely on the ability of an experienced observer to see defects in signatures.

Another approach would be to make repetitive scans of pairs of circuits at the command of an operator and display the differential signal on each scan. The operator could make adjustments to the alignment and the illumination until the differential signal fell within realistic bounds over all or most of its length. This would indicate the presence or absence of defects. If the only way to bring about a near-zero differential signal is to make excessive adjustments to one signature, indicating a gross defect on that circuit, then this can be called to the operator's attention by means of a monitor on the adjustment. None of these ideas have been studied in detail.

CHAPTER VI - REDUCTION TO PRACTICE

The majority of comments in this chapter are related to the reduction to practice of the basic system used in the experimentation. It is the system which has received the most attention and quantitative estimates for the operation of a realistic machine with the capability of detecting defects down to 0.5 mil in diameter can be made with some confidence.

The Equipment

Costs. -- The basic system, exclusive of wafer handling machinery and any automatic focusing and alignment equipment, will cost about $4,250 to build as a commercial unit. The operation of this gear will need human intervention at the beginning of each scan across the wafer and human inspection of all the circuits passed by the machine. It will only act as a pre-screen, rejecting circuits with gross defects. The complementary version could be made, with the decision criteria set so that the machine only accepts circuits within close tolerances. Then the operator would need to screen only those circuits rejected. The level of confidence in this second type of system is less than the first system; the operator may end up inspecting most of the circuits anyway. By using a slightly more complex signal processing system, the circuits could be sorted into bins, the extreme grades being "definitely accept" and "definitely reject." Then the operator need only look at the circuits in the intervening bins, starting in detail with the "probably accept" and only giving a cursory examination to the "probably reject."

The cost of mechanical handling gear for a system of this type will depend greatly on the features needed. Gear of the type used in wafer probe applications is not entirely suitable; it will need modification to allow for adjustment down to a few microinches before each scan and then a smooth scan across each wafer. However, the cost of a commercial version of the wafer handling gear suitable for visual inspection is likely to be approximatley the same as the cost for the wafer probe machinery.

The cost of an automatic alignment and focusing system has not been considered in detail. Special features on the circuits must be made to do this. If such a system is desired, it should not cost more than $2,000 or $3,000, using a laser interferometric system.

The cost estimates for the basic parts of the system are based on direct experience of the cost of the components needed to make the experimental unit. The cost estimates for the other parts of the system are based on direct comparison with the cost of similar equipment available elsewhere. The estimates are summarized in Table XIII.

Inspection Rate. -- The inspection rate of a system of this type will depend on the precise mode of use. The system has already operated during the demonstration plan at about 10s per scan per circuit. Since two scans were needed for 100% inspection of each circuit, this was equivalent to 20s per circuit. There is no reason to doubt that this can be improved to 1s per circuit per scan just by changing the motor drive. This was not done because of the bandwidth limitation on the chart recorders. Since two circuits are inspected every scan, this means that during the demonstration two circuits were inspected, using two scans of total time 20s. The goal in the contract of two circuits per second is within sight. More complex handling equipment with suitable wide band photo-detectors and electronics should allow inspection rates up to 10 circuits per second. There is no fundamental limit to the inspection rate in the basic system concept. However, these rates only represent the continuous scan phase of the inspection. Alignment, whether manual or automatic, is necessary at the beginning of each scan and if no special features are provided on the circuits for this purpose, this may take up to two minutes. This is one adjustment per row of 20 to 50 circuits. However, it must be made more than once (twice in our example) for 100% inspection coverage. If fiduciary marks are provided, the alignment time, especially for the automated system, is reduced to a few seconds. Two other features to consider are the possibility of checking the alignment and focus automatically on each circuit during the scan (a few seconds each time if done automatically with the aid of fiduciary marks), and the need for the operator to inspect many of the circuits after the preliminary machine inspection to bring the efficiency of the inspection to the desired high level. Human inspection takes 15 to 30s per circuit. Therefore, with this the inspection rate per circuit is still of the order of 30s. However, if the preliminary automatic inspection works efficiently within carefully defined limits, there should be no need for the human inspector to inspect all the circuits on a wafer so the mean time per circuit, weighted to the total number of circuits on the wafer, is less than this (See Table XIV.).

Since the operator is still playing a significant role in the system being discussed here, the major costs for inspection will be associated with the operator and can be estimated from figures of the type given in Table XIV, together with typical hourly rates for an operator. It appears that inspection should

TABLE XIII

COST ESTIMATES FOR A SIMPLE AUTOMATED VISUAL INSPECTION SYSTEM

Basic System:		
	Major optical components	$ 1,300
	Light source	250
	Optical filters	100
	Fiber optic pick-ups	100
	Photo-detectors	50
	Electronic signal processor	100
	Power supplies	700
	Stage	320
	Motor drive	30
	Mechanical fixtures	300
	Display	1,000
	TOTAL	$ 4,250
Other Features:		
	Mechanical handling equipment	$ 7,000
	Automatic alignment and focus	1,500
	Digital storage (disc)	9,000
	Digital data processing	5,000
	Equipment for logging defects	1,000
	GRAND TOTAL	$ 27,750

TABLE XIV

ESTIMATES OF INSPECTION RATE

Assumptions

A wafer with 25 rows averaging 20 circuits per row; two scans per circuit for 100% inspection; 1 second per scan per circuit.

Basic scan time for 500 circuits:	1,000s
Manual alignment for 40 scans	4,800s
Total inspection time with no operator verification, 500 circuits:	5,800s
Manual inspection for 50 circuits:	1,000s
Total inspection time with operator verification of 10% of circuits:	6,800s
Manual inspection for 250 circuits:	5,000s
Total inspection time with operator verification of 50% of circuits:	10,800s
Automatic alignment for 40 scans:	200s
Total inspection time with automatic alignment and no operator verification, 500 circuits	1,200s
Total inspection time with automatic alignment and operator verification of 50% of circuits:	6,200s

cost about 1¢ per circuit. The equipment itself should need little maintenance and the only spares required are lamps for the illuminator (a few cents per hour).

The closely related cost and time estimates indicate quite clearly the need to reduce human participation in the operation of the equipment. Using it as an operator's aid does somewhat reduce the number of circuits to be scanned by an operator and hopefully makes the operator more efficient at examining those circuits which must be inspected visually.

Table X gives information on the reliability of the system developed. A machine based on the experimental gear but with all the improvements suggested would be able to detect smaller defects with a 100% confidence level.

Other Applications. -- In principle there should be little difference in the automatic inspections of normal IC's, MSI or LSI. In practice there will be some difference because of the narrower lines and the higher component densities characteristic of these circuit types. On a circuit with 1 mil metallization width, a void of 0.1 mil dimension may be acceptable, but it is a catastrophic defect on an LSI circuit with 0.1 mil metallization widths. Therefore, it becomes more important to be able to detect small defects with confidence. Discretionary wired circuits cannot be inspected in this way, since there is no master against which to compare the circuits.

The inspection scheme which has been developed can be applied to any sequence of iterative patterns. It can be applied with equal facility to all aspects of the integrated circuit fabrication, including the wafers, the masks, the photoresist, the diffusion, and the metallization steps. With suitable handling equipment it can also be applied to the pre-cap visual inspection. The cost of this type of equipment is likely to be much higher than for wafer handling equipment. Also, alignment must be done before each circuit so the scan rate is reduced by this factor.

Discussion

Obviously, these costs given here are only basic costs and they are applicable to the more sophisticated systems discussed in Chapter V. However, it is necessary to add the cost of the more sophisticated items such as analog to digital converters, data storage, etc.. A single optical channel machine with digital data storage and limited computational power will probably require an extra $10,000 to purchase the extra subsystems.

The optical, mechanical, and electrical features of an automated visual inspection scheme are now well-established. The equipment, whatever the precise design, will operate more efficiently if fiduciary marks are provided for alignment and focusing on each circuit. Two disks, placed in diagonally opposed corners on each circuit, will be satisfactory as fiduciary marks. The disks should have a good contrast against the background oxide. A suitable diameter for the disks is the width of the metallization on the circuit and their placement should leave a width of oxide approximately equal to one disk diameter between the scribe channels and the disk. If inspection is to be done at several stages during the production process, the disks must be indicated on each mask in the production set.

APPENDIX A

THE DESIGN REVIEW MEETING

A design review meeting was held at Arthur D. Little, Inc., on June 16, 1970. Those present were Messrs. Frazer, Reynolds, Sung and Wright of the Jet Propulsion Laboratory, Messrs. Liimattainen, Pauplis and Watt of NASA/ERC and Messrs. Curtis and Lorah of Arthur D. Little, Inc. An extensive discussion of the results of the experimental work performed during the contract, the design of the experimental apparatus and the modification suggested in Chapter V of this report was held. As a direct result the following action items were agreed upon.

1. Discuss in the report the limits on the allowable angle between the image plane and the plane of the mask carrying the slits, see page 29.

2. Discuss in the report the limits on the scan rate, see page 27.

3. Recommend in the report the fiduciary marks required to aid in automatic alignment, see page 79.

4. Add extra data concerning the probable cost of equipment for logging defects and displaying the information.

5. Discussions will be held on the possibility of developing further the inspection equipment.

6. List in the report the action items agreed upon at the meeting, this appendix.

APPENDIX B

New Technology

1. Improved optical filters for the automated inspection equipment.

   Described on pages 32 - 35 this report

2. An apparatus to assist in the alignment of microcircuits in the automated visual inspection equipment.

   Not described in detail in this report. The improvement consisted of making each slit on an opaque area in the center of a transparent mask carrying a scale so that the experimenter can align the circuits. Later experience showed that the alignment performed in this manner was not sufficiently accurate.

3. An adjustable pair of slits.

   Not described in this report. In order to utilize fully an automated alignment equipment with circuits of many different sizes, there must be some means of adjusting the spacing between the slits on the mask. A system of this type was not made.